

8-1-2023

CSF MTBR-tau243 is a specific biomarker of tau tangle pathology in Alzheimer's disease

Kanta Horie
Washington University School of Medicine in St. Louis
Nicolas R Barthélemy
Washington University School of Medicine in St. Louis
Yan Li
Washington University School of Medicine in St. Louis
Yingxin He
Washington University School of Medicine in St. Louis
Benjamin Saef
Washington University School of Medicine in St. Louis

See next page for additional authors

Follow this and additional works at: https://digitalcommons.wustl.edu/oa_4



Part of the [Medicine and Health Sciences Commons](#)

Please let us know how this document benefits you.

Recommended Citation

Horie, Kanta; Barthélemy, Nicolas R; Li, Yan; He, Yingxin; Saef, Benjamin; Chen, Charles D; Jiang, Hong; Sato, Chihiro; Gordon, Brian A; Benzinger, Tammie L S; Holtzman, David M; Morris, John C; Schindler, Suzanne E; Bateman, Randall J; and et al., "CSF MTBR-tau243 is a specific biomarker of tau tangle pathology in Alzheimer's disease." *Nature Medicine*. 29, 8. 1954 - 1963. (2023).
https://digitalcommons.wustl.edu/oa_4/2166

This Open Access Publication is brought to you for free and open access by the Open Access Publications at Digital Commons@Becker. It has been accepted for inclusion in 2020-Current year OA Pubs by an authorized administrator of Digital Commons@Becker. For more information, please contact vanam@wustl.edu.

Authors

Kanta Horie, Nicolas R Barthélemy, Yan Li, Yingxin He, Benjamin Saef, Charles D Chen, Hong Jiang, Chihiro Sato, Brian A Gordon, Tammie L S Benzinger, David M Holtzman, John C Morris, Suzanne E Schindler, Randall J Bateman, and et al.












CSF MTBR-tau243 is a specific biomarker of tau tangle pathology in Alzheimer's disease

Received: 2 January 2023

Accepted: 5 June 2023

Published online: 13 July 2023

 Check for updates

Kanta Horie ^{1,2,3,13}, Gemma Salvadó ^{4,13}, Nicolas R. Barthélemy^{1,2}, Shorena Janelidze ⁴, Yan Li², Yingxin He ^{1,2}, Benjamin Saef², Charles D. Chen⁵, Hong Jiang², Olof Strandberg⁴, Alexa Pichet Binette ⁴, Sebastian Palmqvist ^{4,6}, Chihiro Sato ^{1,2}, Pallavi Sachdev³, Akihiko Koyama³, Brian A. Gordon ^{5,7}, Tammie L. S. Benzinger ^{5,7,8}, David M. Holtzman ^{2,7,8}, John C. Morris^{2,7}, Niklas Mattsson-Carlgren^{4,9,10}, Erik Stomrud^{4,6}, Rik Ossenkoppele ^{4,11,12}, Suzanne E. Schindler ^{2,7}, Oskar Hansson ^{4,6,13} ✉ & Randall J. Bateman ^{1,2,7,8,13} ✉

Aggregated insoluble tau is one of two defining features of Alzheimer's disease. Because clinical symptoms are strongly correlated with tau aggregates, drug development and clinical diagnosis need cost-effective and accessible specific fluid biomarkers of tau aggregates; however, recent studies suggest that the fluid biomarkers currently available cannot specifically track tau aggregates. We show that the microtubule-binding region (MTBR) of tau containing the residue 243 (MTBR-tau243) is a new cerebrospinal fluid (CSF) biomarker specific for insoluble tau aggregates and compared it to multiple other phosphorylated tau measures (p-tau181, p-tau205, p-tau217 and p-tau231) in two independent cohorts (BioFINDER-2, $n = 448$; and Knight Alzheimer Disease Research Center, $n = 219$). MTBR-tau243 was most strongly associated with tau-positron emission tomography (PET) and cognition, whereas showing the lowest association with amyloid-PET. In combination with p-tau205, MTBR-tau 243 explained most of the total variance in tau-PET burden ($0.58 \leq R^2 \leq 0.75$) and the performance in predicting cognitive measures ($0.34 \leq R^2 \leq 0.48$) approached that of tau-PET ($0.44 \leq R^2 \leq 0.52$). MTBR-tau243 levels longitudinally increased with insoluble tau aggregates, unlike CSF p-tau species. CSF MTBR-tau243 is a specific biomarker of tau aggregate pathology, which may be utilized in interventional trials and in the diagnosis of patients. Based on these findings, we propose to revise the A/T/(N) criteria to include MTBR-tau243 as representing insoluble tau aggregates ('T').

Given the growing interest in tau-targeted therapeutics for Alzheimer's disease (AD), there is a critical need for reliable and specific biomarkers of insoluble, aggregated tau to understand AD pathophysiology and to evaluate the effects of treatments¹. PET with radio ligands that bind to fibrillar forms of tau reflect the burden

of insoluble AD-specific tau aggregates in the brain, including neurofibrillary tangles (NFTs) and neuropil threads^{2–6}. Tau-PET imaging studies have shown that insoluble tau aggregates are strongly associated with cognitive decline even during the early pre-symptomatic stages of AD⁷ and tau-PET is the most accurate prognostic marker of

A full list of affiliations appears at the end of the paper. ✉ e-mail: oskar.hansson@med.lu.se; batemanr@wustl.edu

AD available today⁸; however, PET imaging is highly expensive and needs a complex infrastructure, which reduces its use to only highly specialized centers. In contrast, fluid biomarkers are less expensive and are more clinically accessible. The most widely used fluid biomarkers of tau are N-terminal or mid-domain total tau (t-tau) and phosphorylated tau species resulting from cleavage near residue 224 of tau^{9,10}, including tau phosphorylated at residues 181, 217 and 231 (p-tau181, p-tau217 and p-tau231) (refs. 11–17). But, these biomarkers are strongly associated with increasing burden of amyloid plaques more than insoluble tau aggregates^{18–20}. For instance, plasma and CSF concentrations of these p-tau species are already increased in preclinical AD many years before widespread insoluble tau aggregates in the neocortex are observed^{21–24}. Further, recent clinical trials have demonstrated substantial reductions of CSF or plasma concentrations of t-tau, p-tau181 and p-tau217 (refs. 25–28) in response to anti-amyloid passive immunotherapies, which substantially remove amyloid plaques. Neuropathological and imaging studies have also reported strong associations between these fluid biomarkers and amyloid plaques^{19,20,29}. In addition, animal studies have found that CSF t-tau and p-tau are increased in mouse models with amyloid β ($A\beta$) pathology, even when no aggregated tau pathology is observed^{23,30–32}. Taken together, these findings indicate that plasma and CSF concentrations of N-terminal to mid-domain t-tau and p-tau do not directly represent insoluble tau aggregates, but rather reflect a response to amyloid plaque pathology. Thus, there is currently no fluid biomarker that specifically reflects AD-related tau pathology.

In this study, we therefore evaluated a new CSF biomarker of insoluble tau aggregates. Notably, tau species that contain MTBR-tau are a major component of insoluble tau aggregates in the brain^{33–37}, but these fragments have been poorly investigated as candidate biomarkers. In an initial study, with a small sample size of controls and AD patients ($n = 35$), we showed preliminary results that MTBR-tau was present in human CSF and that a specific MTBR-tau species containing residue 243 (MTBR-tau243) was strongly associated with tau-PET and disease progression³³. Here, we expanded these results to two large independent sporadic AD cohorts, the Swedish BioFINDER-2 study and the Charles F and Joanne Knight Alzheimer Disease Research Center (Knight ADRC), covering the whole AD continuum, with available amyloid-PET and tau-PET images. In this study, we compared the performance of MTBR-tau243 to other CSF phosphorylated tau measures, including p-tau181, p-tau205, p-tau217 and p-tau231 phosphorylation occupancies (% p-tau to total tau ratio), which are also reported as biomarkers to recapitulate AD pathologies^{21,29} and we showed that MTBR-tau243 was the fluid biomarker most strongly associated with tau-PET. We also investigated the proportion of variation in CSF biomarker levels explained by amyloid-PET and tau-PET measures of pathology. Then, we evaluated longitudinal CSF biomarker changes to investigate their rate of change based on the presence or absence of amyloid and tau pathologies to indicate which are increasing with amyloid versus tau pathologies. Finally, we assessed whether prediction of continuous AD-related measures could be improved by the combination of multiple biomarkers and found that MTBR-tau243, together with p-tau205, could optimally predict tau-PET measures and cognitive impairment.

Results

Participants characteristics

The BioFINDER-2 cohort included 448 individuals, the majority of whom had cognitive impairment (281, 63%): 81 cognitively unimpaired $A\beta$ negative (CU⁻), 79 cognitively unimpaired $A\beta$ positive (CU⁺), 90 $A\beta$ positive with mild cognitive impairment (MCI⁺), 102 $A\beta$ positive with AD dementia (AD⁺) and 96 with other dementias (non-AD) (Table 1). The average age was 70.9 ± 8.4 years (mean \pm s.d.), 221 (49.3%) were women and 258 (57.6%) were *APOE* $\epsilon 4$ carriers. The Knight ADRC cohort included 219 individuals, most of whom were cognitively

unimpaired (171, 78%): 83 CU⁻, 88 CU⁺, 35 very mild AD and 13 AD⁺. The average age was 71.2 ± 6.6 years, 112 (51.1%) were women and 96 (43.8%) were *APOE* $\epsilon 4$ carriers (Extended Data Table 1). CSF biomarkers were measured in the BioFINDER-2 and the Knight ADRC cohorts, including MTBR-tau243 concentration, as well as the phosphorylation occupancy at different tau residues (percent pT181/T181, pT205/T205, pT217/T217 and pT231/T231). The phosphorylation occupancy represents the percentage of soluble tau phosphorylated at a certain amino acid position (Methods), which is a more specific measure of phosphorylation not confounded with total tau concentrations and superior to the corresponding p-tau concentration in prediction of abnormal $A\beta$ status^{29,38}. In Extended Data Fig. 1 and Supplementary Table 1, we compared the CSF levels of all biomarkers in all diagnostic groups in the BioFINDER-2 cohort. We observed that MTBR-tau243 concentrations were not increased in other non-AD tauopathies such as progressive supranuclear palsy or frontotemporal dementia (FTD), thus suggesting a high specificity for AD-related tau. Further, we did not observe any significant difference between MTBR-tau243 concentrations in CU⁺ compared to CU⁻. Of note, we found that two outliers (one in CU⁻ and the other in FTD) that had very high levels of MTBR-tau243 were MAPT R406W mutation carriers who were amyloid negative, but clearly tau-PET positive (indicated in Extended Data Fig. 1).

Association between CSF marker and amyloid or tau measure

CSF MTBR-tau243, pT181/T181, pT205/T205, pT217/T217 and pT231/T231 were assessed for association with amyloid-PET and tau-PET measures of pathology using linear regression models adjusting for age and sex. All participants were compared, in addition to the amyloid-positive-only subgroup, to separate out amyloid from tau pathology effects (Fig. 1). The phosphorylation occupancy at T217 (pT217/T217) was the CSF measure most strongly correlated with amyloid-PET (BioFINDER-2, $\beta = 0.81$, 95% confidence interval (CI) 0.74–0.88; Knight ADRC, $\beta = 0.87$, 0.79–0.95; all $P < 0.001$; Fig. 1a and Extended Data Table 2). MTBR-tau243 concentration was the CSF measure most strongly associated with tau-PET in all participants (BioFINDER-2, $\beta = 0.85$, 0.80–0.90; Knight ADRC, $\beta = 0.76$, 0.65–0.87; all $P < 0.001$) and in amyloid-positive participants (BioFINDER-2, $\beta = 0.84$, 0.77–0.91; Knight ADRC, $\beta = 0.76$, 0.63–0.89; all $P < 0.001$; Fig. 1b and Extended Data Table 2). Notably, the CSF MTBR-tau243 concentration was significantly more strongly associated with tau-PET when compared to pT217/T217 (BioFINDER-2, $\beta = 0.77$, 0.71–0.83, $P_{\text{comp}} < 0.001$; Knight ADRC, $\beta = 0.61$, 0.49–0.73, $P_{\text{comp}} < 0.001$) in all participants and in amyloid-positive participants (BioFINDER-2, $\beta = 0.76$, 0.69–0.84, $P_{\text{comp}} = 0.001$; Knight ADRC, $\beta = 0.58$, 0.43–0.73, $P_{\text{comp}} = 0.001$; Extended Data Table 2). Scatter-plots for the associations of all CSF tau biomarkers and amyloid-PET and tau-PET in both cohorts are shown in Extended Data Figs. 2 and 3, respectively.

We also investigated correlations of CSF tau measures with CSF $A\beta_{42/40}$. Of the CSF tau measures, pT217/T217 was most strongly correlated with CSF $A\beta_{42/40}$ (BioFINDER-2, $\beta = -0.80$, 95% CI -0.86 to -0.74 ; Knight ADRC, $\beta = -0.88$, -0.95 to -0.81 ; all $P < 0.001$; Supplementary Fig. 1 and Supplementary Table 2). In contrast, MTBR-tau243 concentration showed significantly lower association with CSF $A\beta_{42/40}$ compared to pT217/T217 (BioFINDER-2, $\beta = -0.63$, -0.70 to -0.55 , $P_{\text{comp}} < 0.001$; Knight ADRC, $\beta = -0.59$, -0.71 to -0.47 ; all $P < 0.001$; Supplementary Fig. 1 and Supplementary Table 2).

Correlations of CSF tau measures and tau-PET signal in different Braak regions (entorhinal (Braak I), temporal (Braak III–IV) and neocortical (Braak V–VI)) were also investigated as an additional analysis. Comparisons in the amyloid-positive only group demonstrated that CSF MTBR-tau243 had the highest correlations with all Braak regions (BioFINDER-2, $\beta = 0.85$, 0.84 and 0.76; Knight ADRC, $\beta = 0.83$, 0.84 and 0.76 for each Braak regions, respectively; all $P < 0.001$; Extended Data Fig. 4 and Supplementary Table 3).

Table 1 | BioFINDER-2 participants characteristics

	Overall		CU-		CU+		MCI+		AD+		Non-AD	
	n =	448	n =	81	n =	79	n =	90	n =	102	n =	96
Demographics												
Age, years	448	70.9 (8.4)	81	69.9 (9.7)	79	70.5 (9.5)	90	71.7 (7.3)	102	72.5 (6.9)	96	69.8 (8.7)
Women, n	448	221 [49.3%]	81	40 [49.4%]	79	40 [50.6%]	90	38 [42.2%]	102	57 [55.9%]	96	46 [47.9%]
APOE-ε4 carriers, n	447	258 [57.6%]	81	27 [33.3%]	79	58 [73.4%]	89	65 [72.2%]	102	76 [74.5%]	96	32 [33.3%]
Years of education	443	12.2 (3.7)	81	12.0 (3.2)	79	12.2 (3.4)	89	12.5 (4.6)	101	11.9 (3.9)	93	12.5 (3.5)
CSF Aβ measures												
CSF Aβ42/40	427	0.0687 (0.0293)	81	0.1080 (0.0132)	79	0.0553 (0.0134)	85	0.0492 (0.0130)	100	0.0447 (0.0113)	82	0.0922 (0.0217)
CSF Aβ42/40 positivity, n	427	290 [64.7%]	81	0 [0%]	79	79 [100%]	90	90 [100%]	102	102 [100%]	82	26 [27.1%]
Amyloid-PET and Tau-PET measures												
Amyloid-PET, centiloids	268	38.4 (44.4)	81	-4.5 (9.3)	79	41.6 (36.5)	88	71.6 (35.0)	7	115.0 (23.3)	11	12.6 (25.1)
Amyloid-PET positivity, n	268	148 [33.0%]	81	2 [2.5%]	79	55 [69.6%]	88	79 [87.8%]	7	7 [6.9%]	11	3 [3.1%]
Tau-PET Braak I-IV, SUVR	443	1.53 (0.61)	81	1.17 (0.09)	79	1.23 (0.21)	90	1.51 (0.45)	101	2.40 (0.60)	92	1.17 (0.12)
Tau-PET positivity, n	443	162 [36.2%]	81	1 [1.2%]	79	11 [13.9%]	90	45 [50.0%]	101	101 [99.0%]	92	4 [4.2%]
CSF tau by mass spectrometry												
pT181/T181 (%)	448	26.9 (5.6)	81	22.8 (1.6)	79	27.2 (3.8)	90	29.5 (4.9)	102	32.6 (4.1)	96	21.8 (3.6)
pT205/T205 (%)	448	1.14 (0.45)	81	0.79 (0.14)	79	0.97 (0.28)	90	1.24 (0.41)	102	1.70 (0.32)	96	0.86 (0.24)
pT217/T217 (%)	448	6.56 (4.12)	81	2.78 (0.83)	79	5.71 (2.51)	90	8.02 (3.24)	102	11.90 (2.53)	96	3.44 (1.70)
pT231/T231 (%)	448	12.30 (5.69)	81	7.09 (2.15)	79	12.70 (4.16)	90	14.80 (4.59)	102	17.90 (4.46)	96	8.14 (3.61)
MTBR-tau243 (pg/ml)	448	0.445 (0.424)	81	0.192 (0.089)	79	0.281 (0.165)	90	0.449 (0.279)	102	0.992 (0.502)	96	0.207 (0.139)
Cognitive measures												
MMSE	447	25.8 (4.6)	81	29.1 (1.1)	79	28.8 (1.3)	90	26.8 (1.9)	101	19.8 (4.4)	96	25.8 (4.0)

Data are presented as mean (s.d.). Values in square brackets indicate the % in total number within the group. SUVR, standardized uptake value ratio.

Biomarker variation explained by amyloid and tau pathologies

Next, we evaluated the proportion of variation in CSF biomarkers explained by amyloid and tau pathologies. CSF biomarker levels were included as the outcome and amyloid-PET and tau-PET were both included as predictors controlling for age and sex, in our models. In the BioFINDER-2 cohort, variance in CSF pT217/T217 levels was significantly better explained by Aβ pathology as assessed with amyloid-PET, than tau (Aβ, partial R^2 (pR^2) = 0.57, 74.7% R^2 versus tau, pR^2 = 0.19, 24.7% R^2 , P_{comp} < 0.001; Fig. 2a and Extended Data Table 3). CSF pT231/T231 (Aβ, pR^2 = 0.46, 76.0% R^2 ; tau, pR^2 = 0.02, 3.3% R^2 , P_{comp} < 0.001) and pT181/T181 (Aβ, pR^2 = 0.32, 55.7% R^2 ; tau, pR^2 = 0.13, 22.0% R^2 , P_{comp} = 0.006) were also significantly better explained by Aβ pathology. In contrast, variance in CSF MTBR-tau243 concentrations were significantly better explained by tau pathology (Aβ, pR^2 = 0.14, 22.3% R^2 ; tau, pR^2 = 0.38, 60.6% R^2 , P_{comp} < 0.001). The contribution of tau and amyloid to CSF pT205/T205 was similar, with the difference between both being non-significant (Aβ, pR^2 = 0.29, 45.4% R^2 ; tau, pR^2 = 0.25, 39.7% R^2 , P_{comp} = 0.657).

Similar trends were observed in the Knight ADRC cohort, although with a greater proportion of variance was explained by Aβ pathology for all CSF biomarkers, likely because this cohort included relatively few individuals with substantial tau pathology (only n = 36 (16.4%) were tau-PET positive). CSF pT217/T217 (Aβ, pR^2 = 0.51, 75.1% R^2 ; tau, pR^2 = 0.14, 19.9% R^2 , P_{comp} < 0.001), pT181/T181 (Aβ, pR^2 = 0.25, 70.1% R^2 ; tau, pR^2 = 0.02, 4.9% R^2 , P_{comp} < 0.001) and pT231/T231 (Aβ, pR^2 = 0.31, 68.8% R^2 ; tau, pR^2 = 0.04, 8.6% R^2 , P_{comp} < 0.001) were better explained by Aβ pathology. In contrast, tau pathology was the major contributor on explaining variance in CSF MTBR-tau243 levels (Aβ, pR^2 = 0.09, 16.0% R^2 ; tau, pR^2 = 0.36, 66.7% R^2 , P_{comp} < 0.001). Of note, pT205/T205

levels were explained similarly by both tau and amyloid (Aβ, pR^2 = 0.27, 45.2% R^2 ; tau, pR^2 = 0.27, 45.4% R^2 , P_{comp} = 0.990; Fig. 2b and Extended Data Table 3).

Because dementia patients of BioFINDER-2 did not undergo amyloid-PET, analyses were repeated in both cohorts with all participants using CSF Aβ42/40 rather than amyloid-PET as the measure of Aβ pathology (Supplementary Fig. 2 and Extended Data Table 3). Levels of CSF pT217/T217 were slightly, but significantly better explained by CSF Aβ42/40 levels than tau-PET (BioFINDER-2, 66.6% R^2 versus 56.5%, P = 0.044; Knight ADRC, 87.6% R^2 versus 28.9%, P_{comp} < 0.001). CSF Aβ42/40 continued to be the major factor associated with CSF pT231/T231 (BioFINDER-2, 69.8% versus 19.1%, P_{comp} < 0.001; Knight ADRC, 84.0% versus 7.0%, P_{comp} < 0.001) and pT181/T181 (BioFINDER-2, 52.9% versus 33.7%, P_{comp} = 0.014; Knight ADRC, 82.8% versus 3.5%, P_{comp} < 0.001). In these models, tau pathology remained the major factor explaining variance in MTBR-tau243 levels (BioFINDER-2, 21.4% versus 75.1%, P_{comp} < 0.001; Knight ADRC, 33.5% versus 63.8%, P_{comp} = 0.014). For pT205/T205, the major contributor was tau pathology (BioFINDER-2, 19.6% versus 66.8%, P_{comp} < 0.001) although the difference was not significant in Knight ADRC (36.5% versus 57.6%, P_{comp} = 0.125).

Longitudinal change in CSF biomarkers

Longitudinal data from the BioFINDER-2 cohort was used to examine changes in CSF biomarkers stratified by amyloid (A) and tau (T) pathology status (+ and -). Characteristics of the 220 participants with longitudinal CSF measurements are described in Supplementary Table 4. Linear mixed models were used to compare CSF longitudinal trajectories among groups (A-/T-, A+/T- and A+/T+) using post hoc pairwise Wilcoxon test when the interaction with

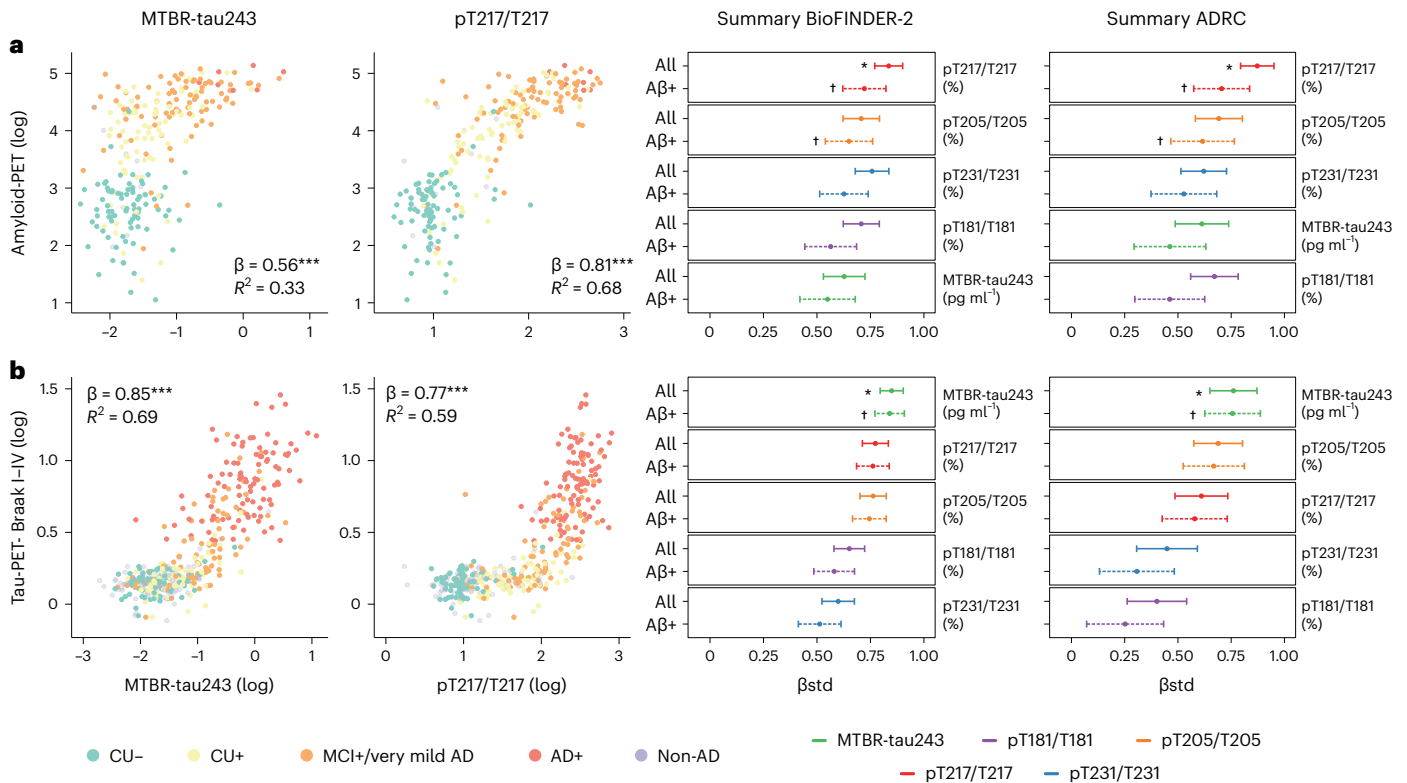


Fig. 1 | Associations between CSF biomarkers and amyloid-PET and tau-PET. **a, b,** Associations between CSF biomarkers and amyloid-PET (**a**) and tau-PET (**b**). First two columns show scatter-plots of MTBR-tau243 (first column) and pT217/T217 (second column) and amyloid-PET ($n = 268$) or tau-PET ($n = 443$) in BioFINDER-2 participants, color-coded by diagnosis and amyloid status. Linear regression models, adjusting for age and sex, were used to obtain β , P values (asterisks) and R^2 shown in the plots. Scatter-plots for all the biomarkers in both cohorts are shown in Extended Data Figs. 1 and 2. The third and fourth columns show standardized β (β_{std}) of the association between each CSF biomarker and amyloid- or tau-PET in BioFINDER-2 and Knight ADRC participants ($n = 219$; except for pT231/T231 in which $n = 184$ for all cases), respectively. Solid and dashed lines show standardized β (central dot) and 95% CI when all participants

or only amyloid-positive participants (BioFINDER-2, amyloid-PET, $n = 172$, tau-PET, $n = 287$; Knight ADRC, $n = 136$; except for pT231/T231 in which $n = 117$) were included, respectively. Asterisks (crosses) show the highest or not significantly different standardized β in all (amyloid-positive only) participants, in each cohort and outcome based on bootstrapping. Thus, those biomarkers without asterisks or crosses have statistically weaker correlations. A β -positive participants were selected based on CSF A β 42/40 previously validated cutoff values (CSF A β 42/40 < 0.08 in BioFINDER-2 and CSF A β 42/40 < 0.0673 in Knight ADRC). Association P values were derived from two-sided tests and bootstrapping P values were obtained from one-sided tests, all without adjustment for multiple comparisons. All P values from associations between CSF biomarkers and amyloid-PET and tau-PET were < 0.001.

time was significant. Amyloid status was derived from CSF A β 42/40 levels and tau was dichotomized from tau-PET measures. Individual and group trajectories over time are shown in Extended Data Fig. 5. CSF pT217/T217, pT181/T181 and pT231/T231 had their greatest rate of increase in the A+T- group and a lower rate of increase in the A+T+ group, indicating that the rate of increase of these biomarkers was plateauing at later stages of disease when tau pathology was increasing most (Fig. 3). In contrast, CSF pT205/T205 and MTBR-tau243 had their greatest rate of increase in the A+T+ group, corresponding to matching increases in tau pathology. Notably, CSF MTBR-tau243 was increasing faster in the A+T+ group than the A+T- group (versus A-T-, Cohen's $d = 1.48$, $P < 0.001$; versus A+T-, Cohen's $d = 1.13$, $P < 0.001$), whereas the rate of increase in pT205/T205 was not significantly different in the A+T+ and A+T- groups (Cohen's $d = 0.08$, $P = 0.788$; Fig. 3 and Supplementary Table 5). This suggests that CSF MTBR-tau243 would best reflect AD progression in tau-PET positive individuals.

As a sensitivity analysis, we repeated this analysis using amyloid-PET rather than CSF A β 42/40 for classifying participants, using a previously validated threshold³⁹. We found that the longitudinal trajectories for all CSF biomarkers were replicated, with pT205/T205, but especially MTBR-tau243, rates of change increasing with progressing A/T status and the rest of biomarkers having the highest

rate of change at A+T- status (Supplementary Fig. 3 and Supplementary Table 5).

Association of CSF and PET biomarkers with MMSE scores

We assessed associations of CSF and PET biomarkers with a common clinical assessment of dementia, the Mini Mental State Examination (MMSE)⁴⁰, which was assessed in both cohorts, using linear regression models that adjusted for age, sex and years of education. MTBR-tau243 was the CSF biomarker most strongly associated with MMSE scores in all participants (BioFINDER-2, $\beta = -0.65$, -0.74 to -0.57 ; Knight ADRC, $\beta = -0.54$, -0.67 to -0.42 , all $P < 0.001$) and amyloid-positive participants (BioFINDER-2, $\beta = -0.56$, -0.66 to -0.46 ; Knight ADRC, $\beta = -0.54$, -0.69 to -0.39 , all $P < 0.001$; Fig. 4 and Supplementary Table 6). These associations were significantly stronger than those of pT217/T217, as assessed by bootstrapping, for all participants (BioFINDER-2, $\beta = -0.60$, -0.69 to -0.52 , $P_{comp} = 0.001$; Knight ADRC, $\beta = -0.40$, -0.53 to -0.26 , $P_{comp} = 0.003$) and amyloid-positive participants (BioFINDER-2, $\beta = -0.48$, -0.59 to -0.38 , $P_{comp} = 0.002$; Knight ADRC, $\beta = -0.36$, -0.52 to -0.19 , $P_{comp} = 0.001$); however, tau-PET was more strongly associated with MMSE than any CSF biomarker (BioFINDER-2, $\beta = -0.73$, -0.79 to -0.64 , $P_{comp} = 0.036$; Knight ADRC, $\beta = -0.64$, -0.74 to -0.53 , $P_{comp} < 0.001$). Scatter-plots for each CSF biomarker are shown in Extended Data Fig. 6.

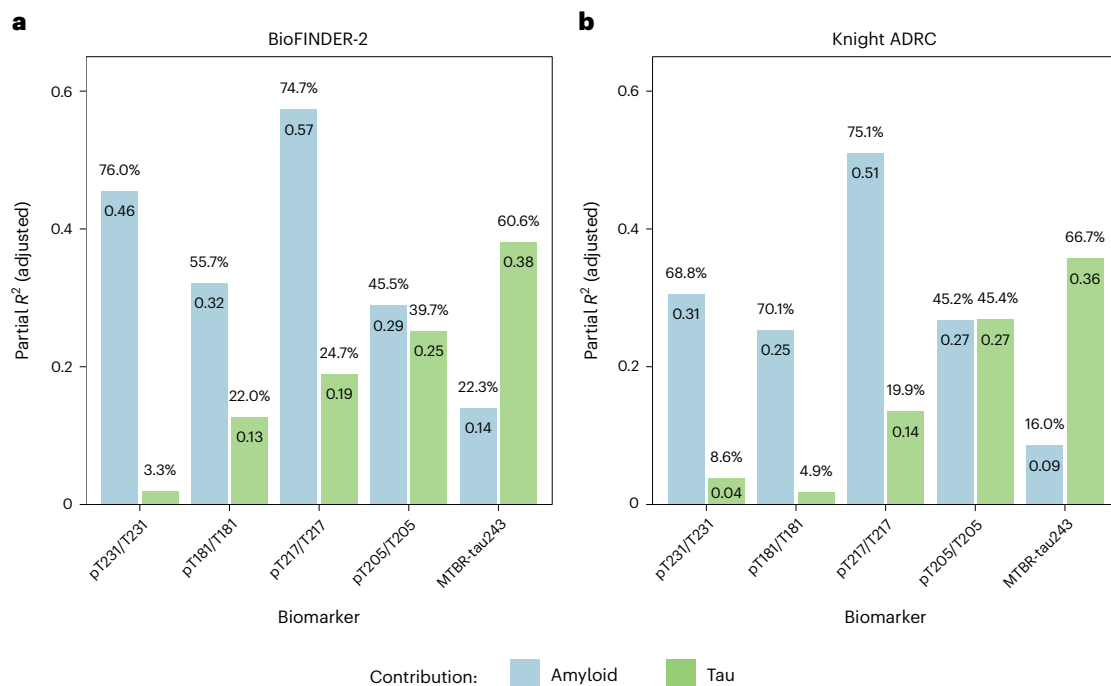


Fig. 2 | Proportion of variation of CSF biomarker levels explained by amyloid-PET and tau-PET. a, b, Partial R^2 values are displayed within the columns and the percentages of partial R^2 over the total R^2 of the model are indicated above each column for BioFINDER-2 (a) and Knight ADRC participants (b). These values were computed using individual CSF biomarkers as outcomes and amyloid and

tau measures as predictors in linear regression models adjusted for age and sex, within each CSF biomarker and cohort. The percentages may not sum up to 100% due to potential shared variance. The biomarkers are arranged from left to right based on the increasing contribution (%) of tau to their levels.

Best predictors of AD-related measures and cognitive function

Finally, we aimed to determine whether combinations of CSF biomarkers could be used as accurate quantitative surrogates for amyloid-PET, tau-PET or cognitive measures. We first evaluated the variance explained by each individual biomarker for each outcome. Next, we used the least absolute shrinkage and selection operator (LASSO) procedure to select which combination of CSF biomarkers were optimal for each outcome and then, we compared this new model to the ones from the individual biomarkers.

CSF pT217/T217 was the individual biomarker that best predicted amyloid-PET (BioFINDER-2, $R^2 = 0.73$, corrected Akaike information criterion (AICc) = 404.5; Knight ADRC, $R^2 = 0.73$, AICc = 265.2; Fig. 5 and Supplementary Table 7). Based on the LASSO regressions, we found that combining CSF pT217/T217 with pT205/T205 and A β 42/40 significantly improved prediction of amyloid-PET in both cohorts (BioFINDER-2, $R^2 = 0.77$, AICc = 370.2, $F = 20.974$, $P < 0.001$; Knight ADRC, $R^2 = 0.73$, AICc = 261.7, $F = 5.266$, $P = 0.006$; Extended Data Table 4).

MTBR-tau243 was the individual biomarker that best predicted quantitative tau-PET (BioFINDER-2, $R^2 = 0.68$, AICc = 715.6; Knight ADRC, $R^2 = 0.51$, AICc = 363.2; Fig. 5 and Supplementary Table 7). The optimal model, which combined MTBR-tau243 and pT205/T205, significantly improved prediction of tau-PET amounts in both cohorts (BioFINDER-2, $R^2 = 0.75$, AICc = 614.1, $F = 116.49$, $P < 0.001$; Knight ADRC, $R^2 = 0.58$, AICc = 339.5, $F = 30.268$, $P < 0.001$; Fig. 5 and Extended Data Table 4).

MTBR-tau243 was the individual biomarker that best predicted MMSE scores (BioFINDER-2, $R^2 = 0.42$, AICc = 790.3; Knight ADRC, $R^2 = 0.30$, AICc = 423.0; Fig. 5 and Supplementary Table 7) and prediction improved when pT205/T205 was added (BioFINDER-2, $R^2 = 0.48$, AICc = 754.6, $F = 27.693$, $P < 0.001$; Knight ADRC, $R^2 = 0.34$, AICc = 415.2; Fig. 5 and Extended Data Table 4). Tau-PET predicted MMSE scores better than a combination of CSF biomarkers, but the difference was not

statistically significant (BioFINDER-2, $R^2 = 0.52$, AICc = 724.9, $z = 0.900$, $P = 0.184$; Knight ADRC, $R^2 = 0.44$, AICc = 385.8, $z = -1.405$, $P = 0.080$, Fig. 5). Results for amyloid-positive only participants demonstrated similar results (Supplementary Fig. 4, Supplementary Table 7 and Extended Data Table 4).

Discussion

In this study, we found that a new CSF biomarker, MTBR-tau243, was strongly associated with tau pathology, whereas it was minimally associated with A β pathology, in two large independent sporadic AD cohorts. We also found that CSF MTBR-tau243 has a significantly higher correlation with cognitive measures than phosphorylated tau measures (for example, pT217/T217 and pT181/T181), which indicates its potential utility in the clinical setting. Further, we found that CSF MTBR-tau243 is the biomarker with the largest rate of increase in participants that are already positive for both amyloid and tau pathologies, suggesting that CSF MTBR-tau243 best reflects disease progression in late stages. We further extended these findings by combining CSF MTBR-tau243 with phosphorylated tau measures to predict A β pathology, tau pathology and cognitive measures in the AD continuum. We found that CSF MTBR-tau243 in combination with pT205/T205 can accurately predict continuous tau-PET measures and has similar predictive accuracy for cognitive measures as tau-PET. Based on these results, our study suggests that CSF MTBR-tau243 may be a viable alternative to tau-PET for use as a pre-screening tool or a tau pathology end point surrogate for clinical trials and also as an accurate diagnostic measure of tau pathology.

Our first objective was to characterize MTBR-tau243 concentration and compare it to four phosphorylated tau measures by looking at their associations with A β and tau pathologies measured by PET. Notably, MTBR-tau243 was the tau biomarker that demonstrated the highest correlation with tau-PET and the lowest correlation with amyloid-PET, not only in the whole group, but also in A β -positive group. This suggests

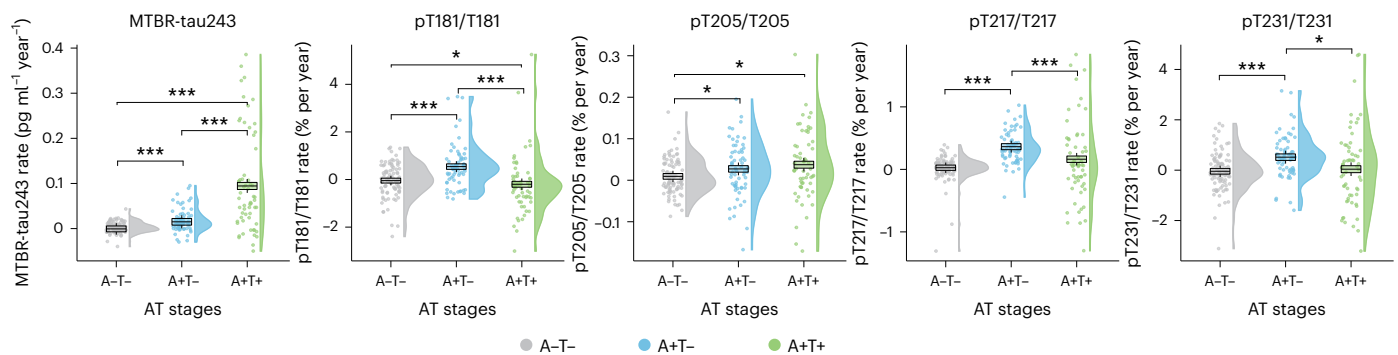


Fig. 3 | Longitudinal CSF biomarkers change by baseline amyloid and tau status. Rates of change in CSF biomarkers per baseline amyloid (A) and tau (T) status are depicted (pT231/T231: $n = 218$, rest: $n = 220$). Individual rates of change are represented by dots. Trajectories for each group are displayed as boxplots, which were generated using linear mixed models (the central band represents the median, the lower and upper hinges correspond to the first and third quartiles and the whiskers depict the maximum/minimum value or $1.5 \times$ interquartile range from the hinge, whichever is lower). Differences among all groups were assessed using Kruskal–Wallis tests and pairwise Wilcoxon tests were employed for post hoc comparisons. Asterisks indicate the P values from two-sided tests without

correction for multiple comparisons. Longitudinal CSF data was available only in BioFINDER-2. Amyloid-positive participants were identified using a previously validated cutoff for CSF A β 42/40 (CSF A β 42/40 < 0.08). Tau positivity was determined based on tau-PET SUVR in the meta-ROI (Braak I–IV, SUVR > 1.32). ROI, region of interest. The actual P values for A–T– versus A+T– were $P = 0.011$ (pT205/T205); for A–T– versus A+T+ were $P = 0.011$ (pT181/T181), $P = 0.014$ (pT205/T205), $P = 0.617$ (pT217/T217) and $P = 0.980$ (pT231/T231); and for A+T– versus A+T+ were $P = 0.788$ (pT205/T205), $P = 0.007$ (pT231/T231). All other comparisons yielded $P < 0.001$. * $P < 0.050$; ** $P < 0.010$; *** $P < 0.001$.

that MTBR-tau243 is a biomarker that specifically reflects aggregated tau pathology independent of amyloid pathology. Although pT217/T217 was also well correlated with tau-PET, there was a nonlinear relationship and a substantial increase in pT217/T217 before tau-PET pathology was elevated, which plateaued once the tau-PET threshold was exceeded. This may indicate that pT217/T217 is primarily associated with tau pathology through its quantitative relationship with the amount of A β pathology. This is further supported by the observation that A β pathology explained a significantly larger proportion of variation of pT217/T217 levels than tau, when including both amyloid-PET and tau-PET measures in the model. Notably, while pT205/T205 levels demonstrated a high correlation with tau-PET, they also showed the second highest correlation with amyloid-PET, after pT217/T217. In combined models, both amyloid-PET and tau-PET explained similar proportion of variation of pT205/T205 levels, suggesting that it is an intermediate biomarker affected by both A β and tau pathologies. Regarding the other p-tau measures, pT181/T181 and pT231/T231 were highly correlated with amyloid-PET, while the correlations with tau-PET were significantly lower than the other three CSF tau biomarkers, suggesting that they mainly reflect A β -pathology. These results are in line with several recent studies suggesting that p-tau181, p-tau217 and p-tau231 may be more related to amyloid pathology than tau. This is supported by their increased levels, both measured in CSF or in plasma, in early stages^{13,14,17,21,22,41–43}, and by being more tightly associated with amyloid-PET than tau-PET^{18,23,44} or to actual amyloid pathology in postmortem studies^{20,45}. Finally, we found that MTBR-tau243 was particularly increased in two cases of MAPT R406W mutation carriers that were amyloid negative but had high tau-PET binding. Tau pathology on MAPT R406W mutation carriers is known to be similar to AD tau pathology^{46,47} and reactive to AD tau-PET tracers^{4,48–50}, further supporting our finding that MTBR-tau243 is a specific biomarker to AD-like tau pathology.

Longitudinal CSF biomarkers changes were also investigated to understand how these biomarkers change at different stages of the disease. Most notably, among the five CSF tau biomarkers, only MTBR-tau243 exhibited a significant increase in the rate of change between A+T– and A+T+ groups, suggesting that it enables longitudinal disease tracking during the phase of the disease characterized by neocortical tau aggregates, which mainly occurs in the symptomatic phase of AD. On the other hand, there was no major difference in the

rate of change between A+T– and A+T+ for pT205/T205, although it still demonstrated a positive rate of changes at this late stage, suggesting a lower but still significant increase after tau deposition. Notably, for the other phosphorylated tau measures (pT181/T181, pT217/T217 and pT231/T231), there was a pronounced increase in the rate of change during the transition from A–T– to A+T–, consistent with a previous report showing that phosphorylated tau (especially p-tau217) is an optimal marker for disease monitoring during the very early (preclinical) stages of the disease⁵¹. Of note, here we found either no significant increase in the rate of change of phosphorylated tau occupancy during the transition from A+T– to A+T+ or a significant decrease in the rate of change, consistent with previous reports²¹. These results suggest that rate of change in these phosphorylated tau measures may plateau or decline at advanced disease stages, when insoluble tau aggregates are depositing in the neocortex, indicating they are discordant longitudinally and that the classic p-tau measures are not direct measures of AD tau pathology⁵². Altogether, the findings of CSF p-tau measures are consistent with previous clinical observational studies and preclinical mouse models^{22,32}, where these biomarkers seem to be driven by A β pathology. These results further support recent proposals to revise the A/T/(N) criteria system, in which any p-tau biomarker can be used as a tau (T) marker⁵³.

As a relevant question for clinical practice, we also investigated the relationship between these CSF biomarkers and a cognitive measure. As expected by the observed associations with tau pathology, MTBR-tau243 was the measure most strongly associated with MMSE, a cognitive test frequently used in the clinical setting. Notably, this association was not significantly different from tau-PET, thus supporting the idea that CSF MTBR-tau243 could be a viable alternative to tau-PET for clinical purposes. Although pT205/T205 had a lower correlation with MMSE than MTBR-tau243, pT205/T205 was also well correlated with MMSE and not significantly different from tau-PET. In contrast, other CSF biomarkers such as pT217/T217 or pT181/T181 showed significantly lower associations.

An unmet need is to determine not just who has amyloid or tau pathology, but if the symptoms are due to those pathologies. Because tau pathology is most highly correlated with cognitive and clinical impairment, an important question is how well CSF biomarkers can predict tau pathology or cognitive impairment. Thus, we next examined whether combining CSF biomarkers would improve prediction of

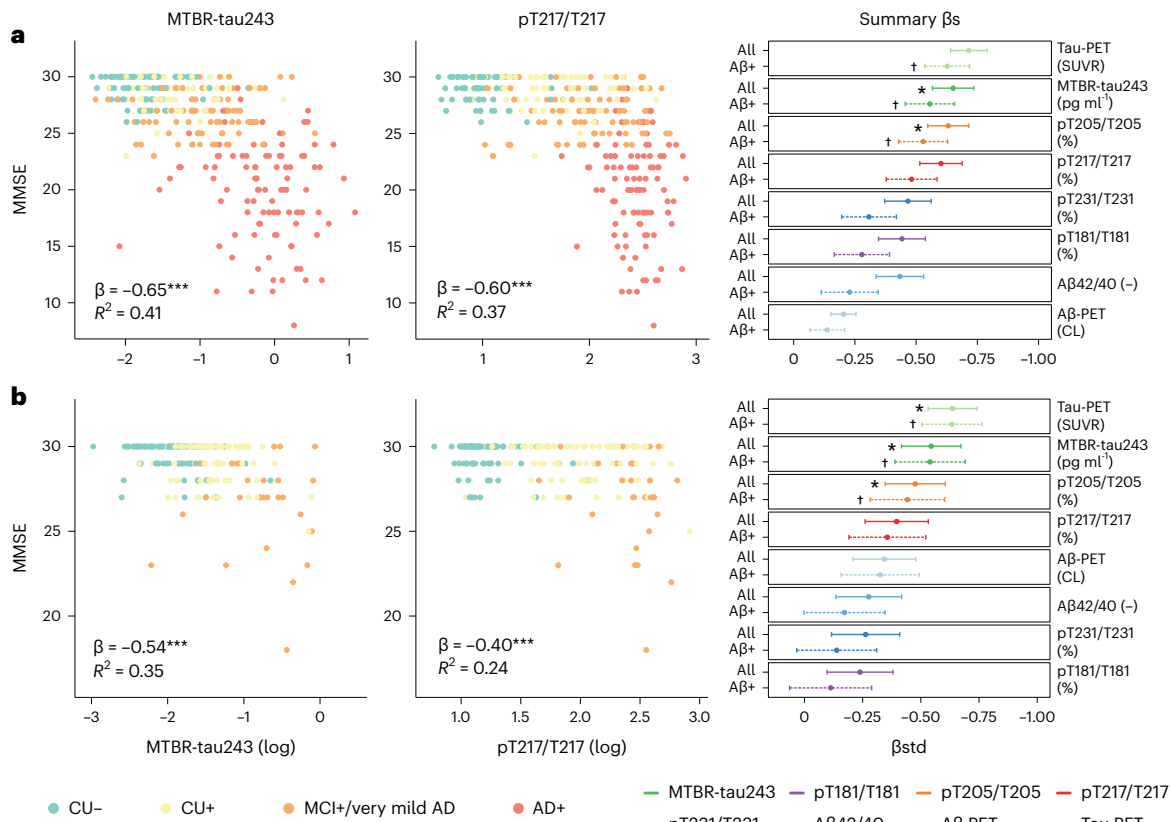


Fig. 4 | Associations between CSF biomarkers and MMSE. a, b, Associations between CSF biomarkers and MMSE are depicted for BioFINDER-2 (a, $n = 342$) and Knight ADRC (b, pT231/T231: $n = 184$, rest: $n = 219$) participants. The first two columns display scatter-plots of MTBR-tau243 (first column) and pT217/T217 (second column) against MMSE, color-coded by diagnosis and amyloid status. In the BioFINDER-2 cohort, orange dots represent MCI+ participants, while in the Knight ADRC cohort, they represent individuals with very mild AD. Linear regression models, adjusted for age, sex and years of education were utilized to obtain β coefficients, P values (asterisks) and R^2 values shown in the plots. Scatter-plots for all biomarkers in both cohorts can be found in Extended Data Fig. 4. The third column shows the standardized β coefficients for all biomarkers, along with the associations of amyloid-PET and CSF A β 42/40 (reversed) and tau-PET for comparison. Solid and dashed lines represent the standardized

β coefficients (central dot) and 95% CI when including all participants or only amyloid-positive participants (BioFINDER-2, $n = 261$; Knight ADRC, $n = 136$, except for pT231/T231, where $n = 117$), respectively. Asterisks (crosses) indicate the highest or not significantly different standardized β coefficients in all (amyloid-positive only) participants within each cohort and outcome, based on bootstrapping. Non-AD participants from BioFINDER-2 were excluded from these analyses. Amyloid-positive participants were selected using previously validated cutoffs for CSF A β 42/40 < 0.08 in BioFINDER-2 and CSF A β 42/40 < 0.0673 in Knight ADRC). Association P values were derived from two-sided tests and bootstrapping p values were obtained from one-sided tests, all without adjustment for multiple comparisons. All p values for associations between CSF biomarkers and MMSE were < 0.001.

A β or tau pathologies or cognitive measures. Based on a data-driven approach, we observed that the combination of pT205/T205, A β 42/40 and pT217/T217 was optimal for predicting amyloid-PET continuous measures and significantly improved the performance of any individual measure. We also found that the combination of MTBR-tau243 and pT205/T205 in a single model improved prediction of tau-PET burden compared to any other single-fluid biomarker. The fact that such high predictive accuracy for both amyloid-PET and tau-PET imaging can be achieved by CSF biomarkers indicates that CSF assays can potentially be an alternative to PET measures, which are costly and have limited accessibility. Notably, MTBR-tau243 and pT205/T205 were also the optimal combination for predicting a cognitive measure (MMSE), suggesting potential clinical applications of this biomarker combination in predicting not only tau pathology but also cognitive impairment. For broader use, the translation of these biomarkers into blood-based biomarkers will be of utmost importance.

The main strength of this study is that we replicated our key findings in two large independent cohorts that represented different types of populations, used different PET tracers and also that we measured collected samples prospectively together with predefined outcome measures. Although further research is needed in a more diverse and

generalizable population to implement our findings in the clinic, it is important to highlight that BioFINDER-2 participants were consecutively recruited from a secondary Clinical Memory in Sweden. As such, this cohort is a representative of memory clinical patients in Sweden and include both AD and also non-AD dementia patients. Limitations include that the magnitude of the trend differed between the two cohorts in some analyses although similar trends were shown. Potential reasons include that the BioFINDER-2 cohort includes more tau-PET-positive participants with AD dementia than the Knight ADRC cohort, as well as more participants in advanced stages of the disease, which may have affected the results with tau-PET and MMSE. Another limitation is that relatively few participants with AD dementia in the BioFINDER-2 cohort had an amyloid-PET scan per study design, although these participants all had CSF A β 42/40. Thus, we used CSF A β 42/40 instead of amyloid-PET as a marker of A β pathology in a sensitivity analysis and confirmed that this limitation did not affect the overall results and interpretations. Further, we acknowledge that our measures of A β and tau pathologies are only surrogate biomarkers and not actual measures of pathology, but both amyloid-PET and tau-PET markers have been validated against neuropathological measures of insoluble A β and tau aggregates, respectively^{2,3,6,54-57}. Future studies

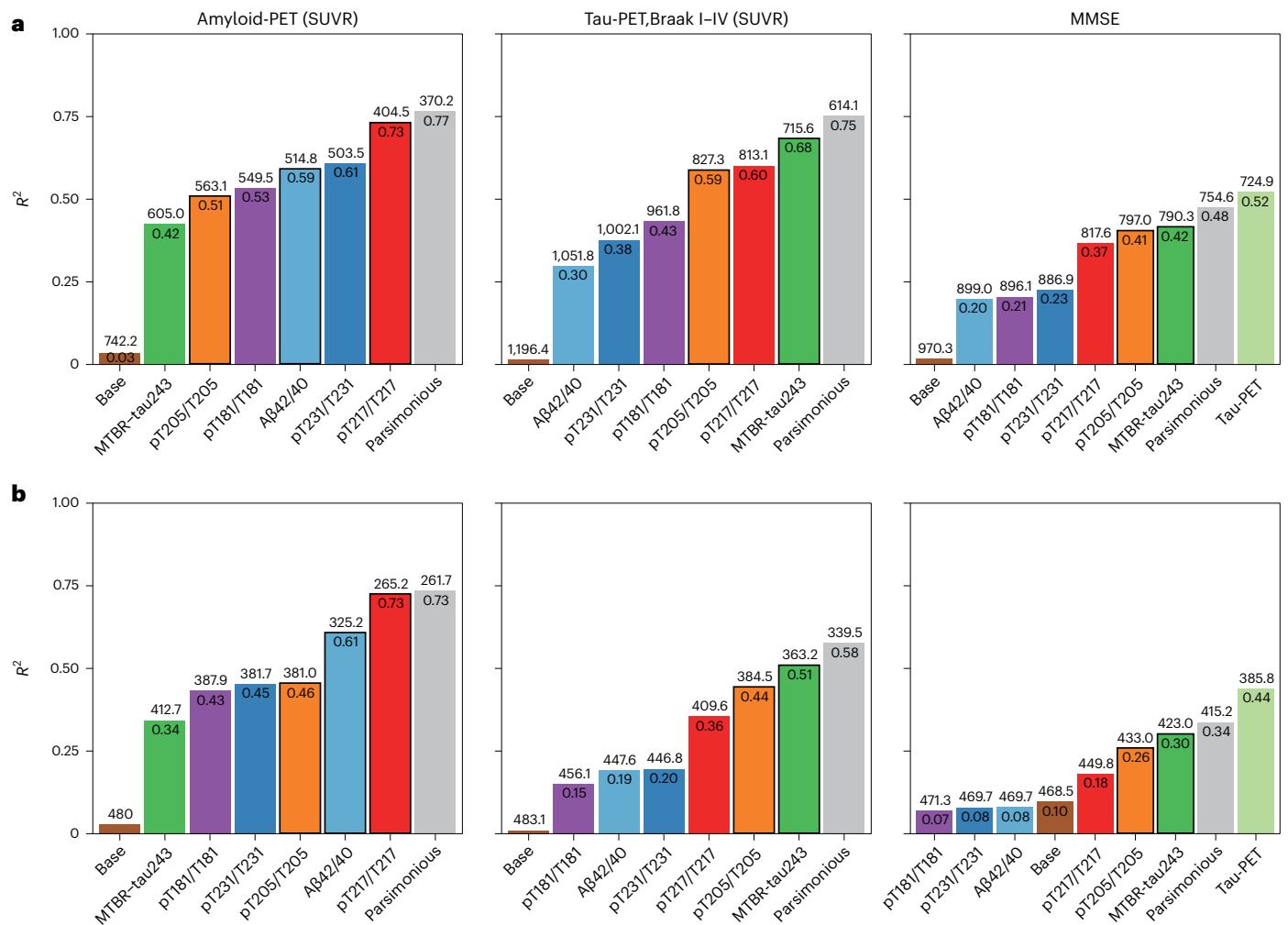


Fig. 5 | Predicting quantitative amyloid-PET, tau-PET and MMSE continuous measures with CSF biomarkers. **a, b.** Linear regression models were employed to predict amyloid-PET (first column, BioFINDER-2, $n = 256$), tau-PET (second column, BioFINDER-2, $n = 422$) and cognition (MMSE, third column, BioFINDER-2, $n = 342$) in BioFINDER-2 (**a**) and Knight ADRC (**b**, $n = 184$). The base model included age and sex (and years of education for MMSE) as predictors. The parsimonious model was derived by using LASSO regression to identify the optimal combination of CSF biomarkers and demographic factors

(age, sex and/or years of education). Biomarkers included in the parsimonious models are indicated by a black border and their names are shown in bold. The other models solely employed individual CSF biomarkers as predictors. For comparison, CSF Aβ42/40 and tau-PET were used as predictors in independent models for predicting all outcomes and cognition only, respectively. Model comparisons were conducted using an *F*-test for nested models or Vuong's test for non-nested models. Non-AD cases were excluded from the BioFINDER-2 cohort for the cognition analyses.

using animal models and neuropathological measures will be important to further validate the results here presented.

In conclusion, these findings confirm that CSF MTBR-tau243 specifically reflects changes in aggregated tau pathology that occur at a late stage of AD progression and are associated with clinical and cognitive symptoms. Thus, we suggest that MTBR-tau243 should replace the commonly used p-tau measures as the fluid biomarker representing insoluble tau aggregate pathology (T) in defining AD pathology and in future versions of the commonly used A/T(N) criteria for AD⁵². As such, MTBR-tau243 could be used to assess AD tauopathy and track the effects of drug treatment independent of amyloid effects. The combination of CSF MTBR-tau243 and pT205/T205 is nearly equivalent to tau-PET measures and predicts MMSE almost as accurately as tau-PET, which indicates clinical utility of a biomarker panel containing MTBR-tau243. Compared to biomarkers altered by amyloidosis that are often abnormal in older cognitively normal individuals, CSF MTBR-tau243 could enable confirmation of tau pathology and provide greater certainty that cognitive symptoms are due to AD, as proposed in the latest clinical AD criteria requiring

biomarker evidence of both amyloid and tau pathology to diagnose AD with high likelihood⁵⁸. These findings add to the improving biomarker diagnostic accuracy for AD and to strategies to develop new AD therapies.

Online content

Any methods, additional references, Nature Portfolio reporting summaries, source data, extended data, supplementary information, acknowledgements, peer review information; details of author contributions and competing interests; and statements of data and code availability are available at <https://doi.org/10.1038/s41591-023-02443-z>.

References

- Ossenkoppele, R., van der Kant, R. & Hansson, O. Tau biomarkers in Alzheimer's disease: towards implementation in clinical practice and trials. *Lancet Neurol.* **21**, 726–734 (2022).
- Smith, R., Wibom, M., Pawlik, D., Englund, E. & Hansson, O. Correlation of in vivo [18f]florotau with postmortem Alzheimer disease tau pathology. *JAMA Neurol.* **76**, 310–317 (2019).

3. Fleisher, A. S. et al. Positron emission tomography imaging with [¹⁸F]flortaucipir and postmortem assessment of Alzheimer disease neuropathologic changes. *JAMA Neurol.* **77**, 829–839 (2020).
4. Smith, R. et al. 18F-AV-1451 tau PET imaging correlates strongly with tau neuropathology in MAPT mutation carriers. *Brain* **139**, 2372–2379 (2016).
5. Soleimani-Meigooni, D. N. et al. 18F-flortaucipir PET to autopsy comparisons in Alzheimer's disease and other neurodegenerative diseases. *Brain* **143**, 3477–3494 (2020).
6. Lowe, V. J. et al. Tau-positron emission tomography correlates with neuropathology findings. *Alzheimers Dement.* **16**, 561–571 (2020).
7. Ossenkoppele, R. et al. Amyloid and tau PET-positive cognitively unimpaired individuals are at high risk for future cognitive decline. *Nat. Med.* **28**, 2381–2387 (2022).
8. Smith, R. et al. Tau-PET is superior to phospho-tau when predicting cognitive decline in symptomatic AD patients. *Alzheimers Dement.* **19**, 2497–2507 (2023).
9. Sato, C. et al. Tau kinetics in neurons and the human central nervous system. *Neuron* **97**, 1284–1298 (2018).
10. Cicognola, C. et al. Novel tau fragments in cerebrospinal fluid: relation to tangle pathology and cognitive decline in Alzheimer's disease. *Acta Neuropathol.* **137**, 279–296 (2019).
11. Barthélemy, N. R., Horie, K., Sato, C. & Bateman, R. J. Blood plasma phosphorylated-tau isoforms track CNS change in Alzheimer's disease. *J. Exp. Med.* <https://doi.org/10.1084/jem.20200861> (2020).
12. Janelidze, S. et al. Plasma P-tau181 in Alzheimer's disease: relationship to other biomarkers, differential diagnosis, neuropathology and longitudinal progression to Alzheimer's dementia. *Nat. Med.* **26**, 379–386 (2020).
13. Palmqvist, S. et al. Discriminative accuracy of plasma phospho-tau217 for Alzheimer disease vs other neurodegenerative disorders. *JAMA* **324**, 772–781 (2020).
14. Thijssen, E. H. et al. Diagnostic value of plasma phosphorylated tau181 in Alzheimer's disease and frontotemporal lobar degeneration. *Nat. Med.* **26**, 387–397 (2020).
15. Karikari, T. K. et al. Blood phosphorylated tau 181 as a biomarker for Alzheimer's disease: a diagnostic performance and prediction modelling study using data from four prospective cohorts. *Lancet Neurol.* **19**, 422–433 (2020).
16. O'Connor, A. et al. Plasma phospho-tau181 in presymptomatic and symptomatic familial Alzheimer's disease: a longitudinal cohort study. *Mol. Psychiatry* **26**, 5967–5976 (2021).
17. Ashton, N. J. et al. Plasma p-tau231: a new biomarker for incipient Alzheimer's disease pathology. *Acta Neuropathol.* **141**, 709–724 (2021).
18. Therriault, J. et al. Association of phosphorylated tau biomarkers with amyloid positron emission tomography vs tau positron emission tomography. *JAMA Neurol.* <https://doi.org/10.1001/jamaneurol.2022.4485> (2022).
19. Mattsson-Carlgrén, N. et al. Soluble P-tau217 reflects amyloid and tau pathology and mediates the association of amyloid with tau. *EMBO Mol. Med.* **13**, e14022 (2021).
20. Salvadó, G. et al. Specific associations between plasma biomarkers and postmortem amyloid plaque and tau tangle loads. *EMBO Mol. Med.* <https://doi.org/10.15252/emmm.202217123> (2023).
21. Barthélemy, N. R. et al. A soluble phosphorylated tau signature links tau, amyloid and the evolution of stages of dominantly inherited Alzheimer's disease. *Nat. Med.* **26**, 398–407 (2020).
22. Milà-Alomà, M. et al. Plasma p-tau231 and p-tau217 as state markers of amyloid-β pathology in preclinical Alzheimer's disease. *Nat. Med.* <https://doi.org/10.1038/s41591-022-01925-w> (2022).
23. Mattsson-Carlgrén, N. et al. Aβ deposition is associated with increases in soluble and phosphorylated tau that precede a positive Tau PET in Alzheimer's disease. *Sci. Adv.* **6**, eaaz2387 (2020).
24. Janelidze, S. et al. Associations of plasma phospho-tau217 levels with tau positron emission tomography in early Alzheimer disease. *JAMA Neurol.* **78**, 149–156 (2021).
25. Pontecorvo, M. J. et al. Association of donanemab treatment with exploratory plasma biomarkers in early symptomatic Alzheimer disease: a secondary analysis of the TRAILBLAZER-ALZ randomized clinical trial. *JAMA Neurol.* <https://doi.org/10.1001/jamaneurol.2022.3392> (2022).
26. Budd Haeberlein, S. et al. Two randomized phase 3 studies of aducanumab in early Alzheimer's disease. *J. Prev. Alzheimers Dis.* **9**, 197–210 (2022).
27. Salloway, S. et al. A trial of gantenerumab or solanezumab in dominantly inherited Alzheimer's disease. *Nat. Med.* **27**, 1187–1196 (2021).
28. van Dyck, C. H. et al. Lecanemab in early Alzheimer's disease. *N. Engl. J. Med.* <https://doi.org/10.1056/NEJMoa2212948> (2022).
29. Barthélemy, N. R. et al. CSF tau phosphorylation occupancies at T217 and T205 represent improved biomarkers of amyloid and tau pathology in Alzheimer's disease. *Nat. Aging* **3**, 391–401 (2023).
30. Schelle, J. et al. Prevention of tau increase in cerebrospinal fluid of APP transgenic mice suggests downstream effect of BACE1 inhibition. *Alzheimer's Dement.* **13**, 701–709 (2017).
31. Maia, L. F. et al. Changes in amyloid-β and tau in the cerebrospinal fluid of transgenic mice overexpressing amyloid precursor protein. *Sci. Transl. Med.* **5**, 194re2 (2013).
32. Kaeser, S. A. et al. CSF p-tau increase in response to Aβ-type and Danish-type cerebral amyloidosis and in the absence of neurofibrillary tangles. *Acta Neuropathol.* **143**, 287–290 (2022).
33. Horie, K., Barthélemy, N. R., Sato, C. & Bateman, R. J. CSF tau microtubule binding region identifies tau tangle and clinical stages of Alzheimer's disease. *Brain* **144**, 515–527 (2021).
34. Roberts, M. et al. Pre-clinical characterisation of E2814, a high-affinity antibody targeting the microtubule-binding repeat domain of tau for passive immunotherapy in Alzheimer's disease. *Acta Neuropathol. Commun.* **8**, 13 (2020).
35. Taniguchi-Watanabe, S. et al. Biochemical classification of tauopathies by immunoblot, protein sequence and mass spectrometric analyses of sarkosyl-insoluble and trypsin-resistant tau. *Acta Neuropathol.* **131**, 267–280 (2016).
36. Shi, Y. et al. Structure-based classification of tauopathies. *Nature* **598**, 359–363 (2021).
37. Fitzpatrick, A. W. P. et al. Cryo-EM structures of tau filaments from Alzheimer's disease. *Nature* **547**, 185–190 (2017).
38. Janelidze, S. et al. Head-to-head comparison of 10 plasma phospho-tau assays in prodromal Alzheimer's disease. *Brain* <https://doi.org/10.1093/brain/awac333> (2022).
39. Binette, A. P. et al. Amyloid-associated increases in soluble tau is a key driver in accumulation of tau aggregates and cognitive decline in early Alzheimer's disease. *Nat Commun.* **13**, 6635 (2022).
40. Folstein, M. F., Folstein, S. E. & McHugh, P. R. "Mini-mental state": A practical method for grading the cognitive state of patients for the clinician. *J. Psychiatr. Res.* **12**, 189–198 (1975).
41. Janelidze, S. et al. Cerebrospinal fluid p-tau217 performs better than p-tau181 as a biomarker of Alzheimer's disease. *Nat. Commun.* <https://doi.org/10.1038/s41467-020-15436-0> (2020).
42. Ashton, N. J. et al. Differential roles of Aβ42/40, p-tau231 and p-tau217 for Alzheimer's trial selection and disease monitoring. *Nat. Med.* <https://doi.org/10.1038/s41591-022-02074-w> (2022).
43. Mielke, M. M. et al. Comparison of plasma phosphorylated tau species with amyloid and tau positron emission tomography, neurodegeneration, vascular pathology, and cognitive outcomes. *JAMA Neurol.* **78**, 1108–1117 (2021).

44. Moscoso, A. et al. Time course of phosphorylated-tau181 in blood across the Alzheimer's disease spectrum. *Brain* **144**, 325–339 (2021).
45. Murray, M. E. et al. Global neuropathologic severity of Alzheimer's disease and locus coeruleus vulnerability influences plasma phosphorylated tau levels. *Mol. Neurodegener.* **17**, 85 (2022).
46. Lindquist, S. G. et al. Alzheimer disease-like clinical phenotype in a family with FTDP-17 caused by a MAPT R406W mutation. *Eur. J. Neurol.* **15**, 377–385 (2008).
47. de Silva, R. et al. An immunohistochemical study of cases of sporadic and inherited frontotemporal lobar degeneration using 3R- and 4R-specific tau monoclonal antibodies. *Acta Neuropathol.* **111**, 329–340 (2006).
48. Wolters, E. E. et al. [18F]Flortaucipir PET across various MAPT mutations in presymptomatic and symptomatic carriers. *Neurology* **97**, e1017–e1030 (2021).
49. Tsai, R. M. et al. 18F-flortaucipir (AV-1451) tau PET in frontotemporal dementia syndromes. *Alzheimers Res. Ther.* **11**, 13 (2019).
50. Jones, D. T. et al. In vivo 18F-AV-1451 tau PET signal in MAPT mutation carriers varies by expected tau isoforms. *Neurology* **90**, e947–e954 (2018).
51. Ashton, N. J. et al. Differential roles of A β 42/40, p-tau231 and p-tau217 for Alzheimer's trial selection and disease monitoring. *Nat. Med.* **28**, 2555–2562 (2022).
52. Jack, C. R. et al. A/T/N: An unbiased descriptive classification scheme for Alzheimer disease biomarkers. *Neurology* **87**, 539–547 (2016).
53. Therriault, J. et al. Association of phosphorylated tau biomarkers with amyloid positron emission tomography vs tau positron emission tomography. *JAMA Neurol.* **80**, 188–199 (2023).
54. Clark, C. M. et al. Cerebral PET with flortbetapir compared with neuropathology at autopsy for detection of neuritic amyloid- β plaques: a prospective cohort study. *Lancet Neurol.* **11**, 669–678 (2012).
55. Sabri, O. et al. Florbetaben PET imaging to detect amyloid beta plaques in Alzheimer's disease: phase 3 study. *Alzheimers Dement.* **11**, 964–974 (2015).
56. Ikonovic, M. D. et al. Post-mortem histopathology underlying β -amyloid PET imaging following flutemetamol F 18 injection. *Acta Neuropathol. Commun.* **4**, 130 (2016).
57. Marquié, M. et al. Validating novel tau positron emission tomography tracer [F-18]-AV-1451 (T807) on postmortem brain tissue. *Ann. Neurol.* **78**, 787–800 (2015).
58. Dubois, B. et al. Clinical diagnosis of Alzheimer's disease: recommendations of the International Working Group. *Lancet Neurol.* **20**, 484–496 (2021).

Publisher's note Springer Nature remains neutral with regard to jurisdictional claims in published maps and institutional affiliations.

Open Access This article is licensed under a Creative Commons Attribution 4.0 International License, which permits use, sharing, adaptation, distribution and reproduction in any medium or format, as long as you give appropriate credit to the original author(s) and the source, provide a link to the Creative Commons license, and indicate if changes were made. The images or other third party material in this article are included in the article's Creative Commons license, unless indicated otherwise in a credit line to the material. If material is not included in the article's Creative Commons license and your intended use is not permitted by statutory regulation or exceeds the permitted use, you will need to obtain permission directly from the copyright holder. To view a copy of this license, visit <http://creativecommons.org/licenses/by/4.0/>.

This is a U.S. Government work and not under copyright protection in the US; foreign copyright protection may apply 2023

¹The Tracy Family SILQ Center, Washington University School of Medicine, St Louis, MO, USA. ²Department of Neurology, Washington University School of Medicine, St. Louis, MO, USA. ³Eisai Inc., Nutley, NJ, USA. ⁴Clinical Memory Research Unit, Department of Clinical Sciences Malmö, Lund University, Lund, Sweden. ⁵Department of Radiology, Washington University School of Medicine, St. Louis, MO, USA. ⁶Memory Clinic, Skåne University Hospital, Malmö, Sweden. ⁷Knight Alzheimer Disease Research Center, Washington University School of Medicine, St. Louis, MO, USA. ⁸Hope Center for Neurological Disorders, Washington University School of Medicine, St. Louis, MO, USA. ⁹Wallenberg Center for Molecular Medicine, Lund University, Lund, Sweden. ¹⁰Department of Neurology, Skåne University Hospital, Lund, Sweden. ¹¹Alzheimer Center Amsterdam, Neurology, Vrije Universiteit Amsterdam, Amsterdam UMC location VUmc, Amsterdam, The Netherlands. ¹²Amsterdam Neuroscience, Neurodegeneration, Amsterdam, The Netherlands. ¹³These authors contributed equally: Kanta Horie, Gemma Salvadó, Oskar Hansson, Randall J. Bateman. ✉e-mail: oskar.hansson@med.lu.se; batemanr@wustl.edu

Methods

Participants

Participants were included from two cohorts: the Swedish BioFINDER-2 (NCT03174938) (ref. 13) at Lund University (Lund, Sweden) and the Knight ADRC from Washington University. The BioFINDER-2 cohort included cognitively unimpaired participants (recruited as cognitively normal controls or as patients with subjective cognitive decline (SCD)), patients with MCI, patients with AD dementia and patients with a non-AD neurodegenerative disease. Participants were recruited at Skåne University Hospital and the Hospital of Ängelholm in Sweden. Details on recruitment, exclusion and inclusion criteria have been presented before¹³. All participants underwent lumbar puncture at baseline and at the follow-up after 2 years for CSF sampling. Participants underwent cognitive testing, including MMSE. The Knight ADRC cohort consisted of community-dwelling volunteers enrolled in studies of memory and aging at Washington University in St Louis. All Knight ADRC participants underwent a comprehensive clinical assessment that included a detailed interview of a collateral source, a neurological examination of the participant, the Clinical Dementia Rating* (CDR)⁵⁹ and the MMSE⁴⁰. Individuals with a CDR of 0.5 or greater were considered to have a dementia syndrome and the probable etiology of the dementia syndrome was formulated by clinicians based on clinical features in accordance with standard criteria and methods⁶⁰.

In the BioFINDER-2 cohort, participants were divided in CU as either A β negative or positive (CU– and CU+, respectively), patients with MCI A β positive (MCI+), patients with AD dementia A β positive (AD+) or patients with non-AD neurodegeneration, regardless of their A β status. Two participants (one in CU– and the other in non-AD) were MAPT R406W mutation carriers with A β negative and tau positive. In the Knight ADRC cohort, participants were divided in CU with CDR of 0 either A β negative or positive (CU– and CU+, respectively), patients with very mild AD with CDR of 0.5 A β positive and patients with AD dementia with CDR \geq 1 A β positive (AD+). In accordance with the research framework by the National Institute on Aging–Alzheimer’s Association study, patients with SCD and cognitively normal controls were considered the CU group⁵. All participants gave written informed consent and ethical approval was granted by the Regional Ethical Committee in Lund, Sweden and the Washington University Human Research Protection Office, respectively.

Anti-tau antibody generation

Antibodies HJ32.11 and HJ34.8 were generated by immunizing tau knockout mice (The Jackson Laboratory) with either keyhole limpet hemocyanin (KLH) fused to amino acids 225–242 of tau to generate antibody HJ32.11 or to KLH fused to amino acids 226–264 to generate antibody HJ34.8. Spleen cells from immunized mice were fused with P3 hybridoma cells and expanded. Clones were screened by direct ELISA.

CSF measurements

Measurement of CSF tau species, including p-tau and MTBR-tau243 was performed at Washington University in both cohorts using the newly developed immunoprecipitation/mass spectrometry (IP/MS) method. We developed two new monoclonal antibodies to immune-purify CSF MTBR-tau243 (HJ32.11, which binds near residue 243 and HJ34.8, which binds near residue 260). The procedure of CSF tau analysis is described in Supplementary Fig. 5. The calculation of percent phosphorylation was performed by measuring the phosphorylated peptide and the non-phosphorylated peptide in the same injection and calculating the percent phosphorylation occupancy as % p-tau/t-tau (ref. 21).

Additionally, CSF A β 42/40 levels were used in both cohorts to assess A β positivity. In the BioFINDER-2 cohort, CSF levels of A β 42/40 were measured as previously explained¹³. A threshold of 0.080, based on a Gaussian mixture modeling, determined A β positivity³⁹. In the Knight ADRC cohort, CSF A β 42/40 levels were measured as explained

previously⁶¹. The threshold (0.0673) had the maximum combined sensitivity and specificity in distinguishing amyloid-PET status.

Imaging acquisition and quantification

In the BioFINDER-2 cohort, amyloid and tau-PET acquiring methods have been previously reported¹³. Briefly, amyloid-PET was acquired using [¹⁸F]flutemetamol and tau-PET using [¹⁸F]RO948. Of note, most of the patients with AD did not undergo amyloid-PET in BioFINDER-2, due to the study design. In the Knight ADRC cohort, participants underwent amyloid-PET using either [¹⁸F]florbetapir ([¹⁸F]AV45) or [¹¹C]PiB and tau-PET with [¹⁸F]flortaucipir ([¹⁸F]AV1451) as previously explained³³. Amyloid-PET was measured in a neocortical meta-ROI using cerebellar gray as a reference region. In the BioFINDER-2 cohort, Centiloids were calculated using the Computational Analysis of PET from AIBL (CapAIBL) pipeline⁶². For tau-PET, SUVRs were calculated using the inferior cerebellum cortex as reference region and binding from a temporal meta-ROI were used for main analyses (Braak I–IV), to capture the regions most affected by tau. In supplementary analyses, we also quantified tau-PET in early (Braak I), intermediate (Braak III–IV) and late (Braak V–VI) regions of tau deposition⁶³. Tau positivity was assessed based on tau-PET in all cases. In the Braak I–IV region, cutoff for positivity was set at SUVR $>$ 1.32 both in BioFINDER-2 and in the Knight ADRC cohorts^{64,65}.

Cognitive tests

MMSE was used as a measure of global cognition in both cohorts.

Statistical analyses

Differences in CSF biomarker levels by diagnostic groups were tested using ANCOVA adjusted for age and sex. Post hoc analyses were performed using the Tuckey test. Linear regression models were used to assess the association between amyloid-PET and tau-PET (independent variable) and each of the CSF biomarkers (dependent variable), after adjusting for age and sex. For cognition, we additionally used years of education as covariate in the linear regression models. All standardized β values were compared to the highest for each outcome and cohort, by building a distribution of the β values’ difference and using that to infer significance using a bootstrapping approach ($n = 500$) with the *boot* package. Proportion of variation of CSF levels by amyloid and tau measures were assessed using linear regression models with both amyloid and tau as predictors, CSF levels as outcomes and age and sex as covariates. We calculated the partial R^2 of amyloid and tau, raw and as a percentage of the total R^2 of the model using the *rsq* package. This was used as a measure of proportion of variance explained by amyloid and tau. Next, prediction of amyloid and tau continuous measures was assessed with linear regression models, where amyloid-PET and tau-PET measures were used as outcomes in independent models and individual CSF biomarkers as predictors. A basic model was also created with only covariates (age and sex) as predictors. Additionally, a parsimonious model was constructed to optimally predict (highest accuracy with lower number of predictors) each of these measures, independently for each cohort. To this aim, LASSO regression models were used (*glmnet* package), initially including all CSF biomarkers and covariates. Only those predictors selected by the LASSO regression and with a significant contribution ($P < 0.1$) in the model were finally included in the parsimonious model. Similar methods were used for predicting cognition (MMSE in the two cohorts and CDR in Knight ADRC) additionally including years of education as covariate. In these cases, we compared the parsimonious model to one including only tau-PET as predictor. F-tests were used to compare nested models (including the same subset of predictors). When comparing models with different predictors we used the Vuong’s test using the *nonnest2* package. Finally, CSF longitudinal changes by baseline amyloid and tau status were assessed in the BioFINDER-2 cohort. Individual participant slopes were calculated using linear regression models to calculate

rate of change differences (mean percentage change) and compare them between groups using a Kruskal–Wallis test. Further, we created group trajectories with linear mixed models using the *lme4* package for visualization. Here, CSF biomarkers were used as outcome, interaction between time and baseline amyloid and tau status as predictor and age and sex main effects as covariates, using random intercepts and fixed time slopes due to low number of time points. CSF and amyloid-PET and tau-PET measures were log-transformed in linear regression analyses. A two-sided *P* value < 0.05 was considered statistically significant. R v.4.1.0 was used for all statistical analyses.

Reporting summary

Further information on research design is available in the Nature Portfolio Reporting Summary linked to this article.

Data availability

The datasets generated and/or analyzed during the current study are available from the corresponding authors (R.J.B. and O.H.). We will share datasets within the restrictions of institutional review board ethics approvals, upon reasonable request. Pseudonymized data from the BioFINDER-2 will be shared by request from a qualified academic investigator for the sole purpose of replicating procedures and results presented in the article and as long as data transfer is in agreement with EU legislation on the General Data Protection Regulation and decisions by the Ethical Review Board of Sweden and Region Skåne, which should be regulated in a material transfer agreement. Knight ADRC data are available to qualified investigators who have a proposal approved by an institutional committee (<https://knightadrc.wustl.edu/Research/ResourceRequest.htm>) that meets monthly. The study must be approved by an institutional review board to ensure ethical research practices and investigators must agree to the terms and conditions of the data use agreement, which includes not distributing the data without permission.

References

- Morris, J. C. The Clinical Dementia Rating (CDR): current version and scoring rules. *Neurology* **43**, 2412a (1993).
- Morris, J. C. et al. The Uniform Data Set (UDS): clinical and cognitive variables and descriptive data from Alzheimer disease centers. *Alzheimer Dis. Assoc. Disord.* **20**, 210–216 (2006).
- Volluz, K. E. et al. Correspondence of CSF biomarkers measured by Lumipulse assays with amyloid PET. *Alzheimers Dement.* **17**, e051085 (2021).
- Bourgeat, P. et al. Implementing the centiloid transformation for 11C-PiB and β -amyloid 18F-PET tracers using CapAIBL. *NeuroImage* **183**, 387–393 (2018).
- Cho, H. et al. In vivo cortical spreading pattern of tau and amyloid in the Alzheimer disease spectrum. *Ann. Neurol.* **80**, 247–258 (2016).
- Leuzy, A. et al. A multicenter comparison of [18F]flortaucipir, [18F]RO948, and [18F]MK6240 tau PET tracers to detect a common target ROI for differential diagnosis. *Eur. J. Nucl. Med. Mol. Imaging* **48**, 2295–2305 (2021).
- Chen, C. D. et al. Comparing tau PET visual interpretation with tau PET quantification, cerebrospinal fluid biomarkers, and longitudinal clinical assessment. *J. Alzheimers Dis.* **93**, 765–777 (2023).

Acknowledgements

This work was supported by resources and effort provided by the Tracy Family SILQ Center (Principal Investigator (PI) R.J.B.) established by the Tracy Family, Richard Frimel and Gary Werths, GHR Foundation, David Payne and the Willman Family brought together by The Foundation for Barnes-Jewish Hospital. This work was also supported by resources and effort provided by the Hope Center

for Neurological Disorders and the Department of Neurology at the Washington University School of Medicine and by the Clinical, Fluid Biomarker and Imaging Cores of the Knight ADRC (P30 AG066444, PI J.C.M., P01 AG03991, PI J.C.M. and P01 AG026276, PI J.C.M.) at the Washington University School of Medicine for participant evaluation, samples and data collection. The mass spectrometry analyses of BioFINDER-2 and Knight ADRC samples were supported by an Eisai industry grant to Washington University (PIs K.H. and R.J.B.) and the Knight ADRC developmental project (PI N.R.B.). Statistical analyses were partially supported by R01AG070941. The Swedish BioFINDER-2 study was by the Swedish Research Council (2016-00906), the Knut and Alice Wallenberg foundation (2017-0383), the Marianne and Marcus Wallenberg foundation (2015.0125), the Strategic Research Area MultiPark (Multidisciplinary Research in Parkinson's disease) at Lund University, the Swedish Alzheimer Foundation (AF-939932), the Swedish Brain Foundation (FO2021-0293), The Parkinson foundation of Sweden (1280/20), the Cure Alzheimer's fund, the Konung Gustaf V:s och Drottning Victorias Frimurarestiftelse, the Skåne University Hospital Foundation (2020-0000028), Regionalt Forskningsstöd (2020-0314) and the Swedish federal government under the ALF agreement (2018-Projekt0279). The precursor of [¹⁸F]-flutemetamol was provided by GE Healthcare and the precursor of [¹⁸F]-RO948 was provided by Roche. The Knight ADRC PET imaging was supported by P30 NS048056. Flortaucipir F18 (AV45) doses were provided by Avid Radiopharmaceuticals, a wholly owned subsidiary of Eli Lilly. Flortaucipir F18 (FTP, T807 and AV1451) was performed at Washington University through technology and materials transfer agreement with Avid Radiopharmaceuticals, a wholly owned subsidiary of Eli Lilly. G.S. received funding from the European Union's Horizon 2020 research and innovation program under the Marie Skłodowska-Curie action grant agreement no. 101061836, from Greta och Johan Kocks research grants and travel grants from the Strategic Research Area MultiPark (Multidisciplinary Research in Parkinson's Disease) at Lund University. We thank the participants and families for their contribution to this study. We also thank the Clinical, Biomarker and Imaging Cores at the Washington University School of Medicine for participant evaluation, samples and data collection. We thank H. Liu, R. Koppiseti, B. Androff, M. Li and C. Hodge for assistance with CSF sample processing and coordination. We thank K. Wildsmith for the project discussion and manuscript review.

Author contributions

K.H., O.H. and R.J.B. conceived the project. K.H. developed the IP/MS method. K.H. and N.R.B. designed MS experiments. H.J. and D.M.H. provided the antibodies for IP. K.H., N.R.B., Y.H. and C.S. executed CSF IP/MS experiments. K.H., G.S., N.R.B., Y.L., B.S., C.D.C., B.A.G., S.E.S., O.H. and R.J.B. analyzed and interpreted the data. O.H. provided mentorship, founded and led Swedish BioFINDER-2 study that enabled recruitment of participants in this study. J.C.M. provided mentorship, founded and led the Knight ADRC that enabled recruitment of participants in this study. S.J. coordinated sample selection at BioFINDER-2 and S.J. and E.S. provided associated data. S.E.S. coordinated sample selection at the Knight ADRC and provided associated data. R.J.B. provided MS resources and mentorship. K.H. and G.S. wrote the initial draft of the paper and contributed equally as first authors. O.H. and R.J.B. supervised the project and contributed equally as senior authors. All authors made substantial contributions to the subsequent version of the manuscript and approved the final version for submission.

Competing interests

K.H. is an Eisai-sponsored voluntary research associate professor at Washington University and has received salary from Eisai. Washington University. R.J.B. and D.M.H. have equity ownership interest in C2N Diagnostics. R.J.B. and D.M.H. receive income from C2N Diagnostics

for serving on the scientific advisory board. K.H., N.R.B., C.S. and R.J.B. may receive income based on technology (Methods to Detect MTBR-tau Isoforms and use Thereof) (PCT/US2020/046224) licensed by Washington University to C2N Diagnostics. H.J. and D.M.H. may receive income based on technology (Anti-tau MTBR Antibodies and Methods to Detect Endogenously Cleaved Fragments of Tau and uses Thereof) (USSN 63/400,345) licensed by Washington University to C2N Diagnostics. R.J.B. is an unpaid scientific advisory board member of Roche and Biogen and receives research funding from Avid Radiopharmaceuticals, Janssen, Roche/Genentech, Eli Lilly, Eisai, Biogen, AbbVie, Bristol Myers Squibb and Novartis. O.H. has acquired research support (for the institution) from ADx, Avid Radiopharmaceuticals, Biogen, Eli Lilly, Eisai, Fujirebio, GE Healthcare, Pfizer and Roche. In the past 2 years, he has received consultancy/speaker fees from AC Immune, Amylyx, Alzpath, BioArctic, Biogen, Cerveau, Eisai, Fujirebio, Genentech, Novartis, Roche and Siemens. S.E.S. has analyzed data provided by C2N Diagnostics to Washington University, but she has not received any research funding or personal compensation from C2N Diagnostics. She has served on a scientific advisory board for Eisai. D.M.H. is on the scientific advisory board of Genentech, Denali and Cajal Neurosciences and consults for Alector. S.P. has served on scientific

advisory boards and/or given lectures in symposia sponsored by BioArctic, Biogen, Cytos, Eli Lilly, Geras Solutions and Roche. The remaining authors declare no competing interests.

Additional information

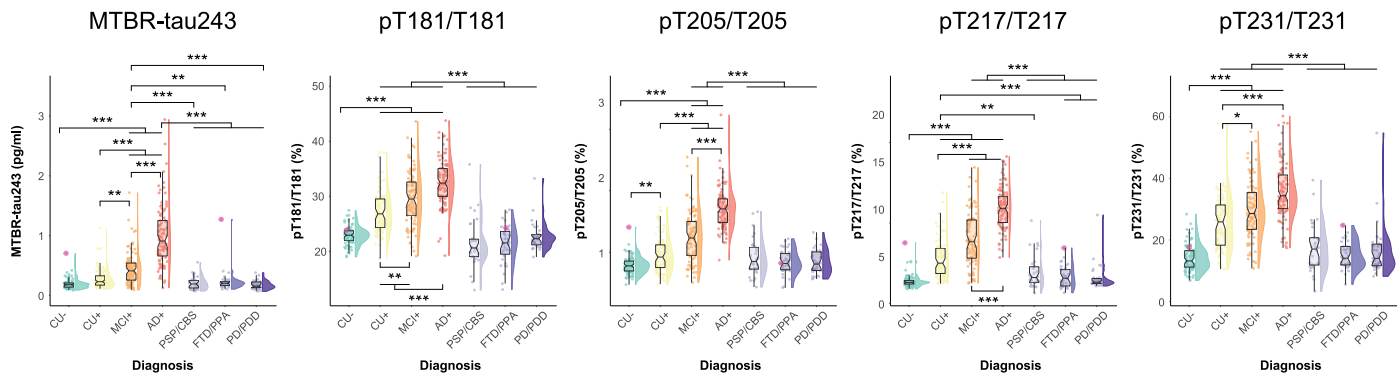
Extended data is available for this paper at <https://doi.org/10.1038/s41591-023-02443-z>.

Supplementary information The online version contains supplementary material available at <https://doi.org/10.1038/s41591-023-02443-z>.

Correspondence and requests for materials should be addressed to Oskar Hansson or Randall J. Bateman.

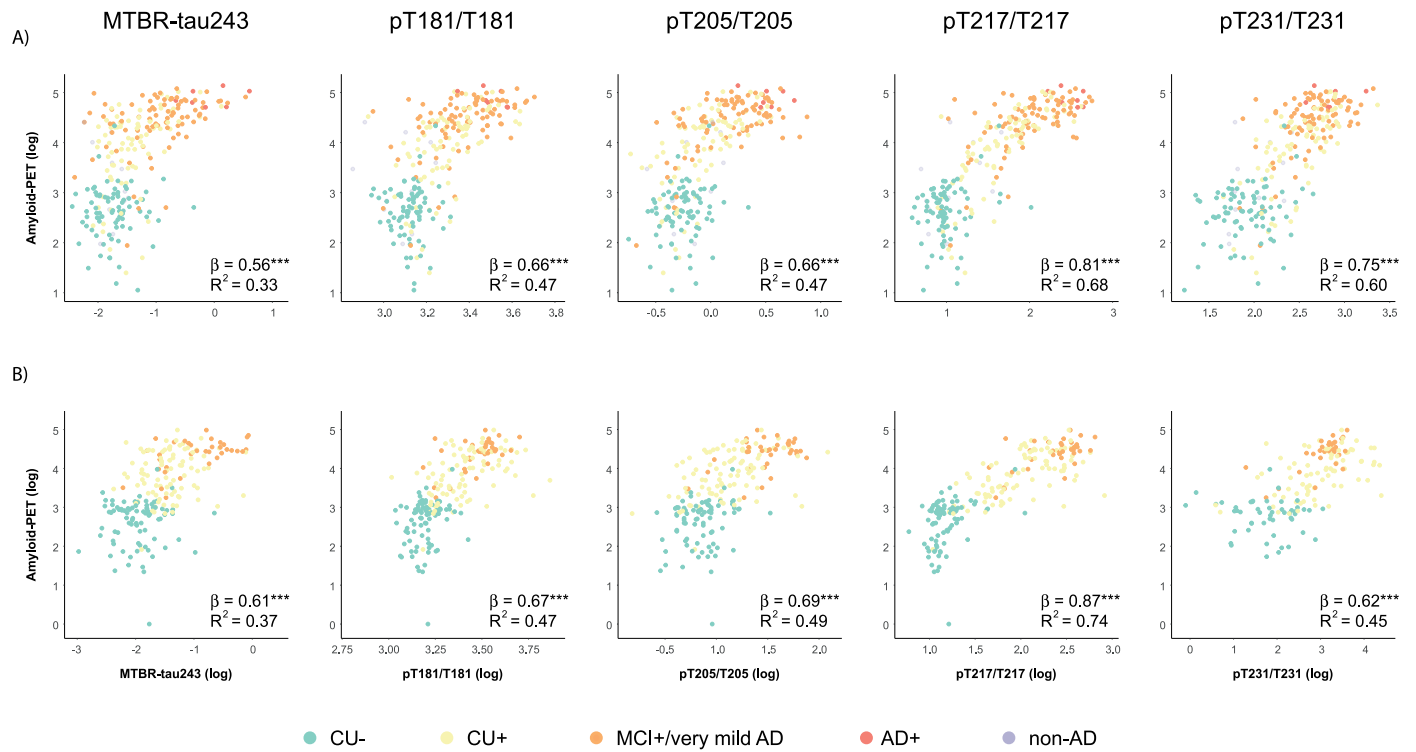
Peer review information *Nature Medicine* thanks Agneta Nordberg and the other, anonymous, reviewer(s) for their contribution to the peer review of this work. Primary Handling Editor: Jerome Staal, in collaboration with the *Nature Medicine* team.

Reprints and permissions information is available at www.nature.com/reprints.



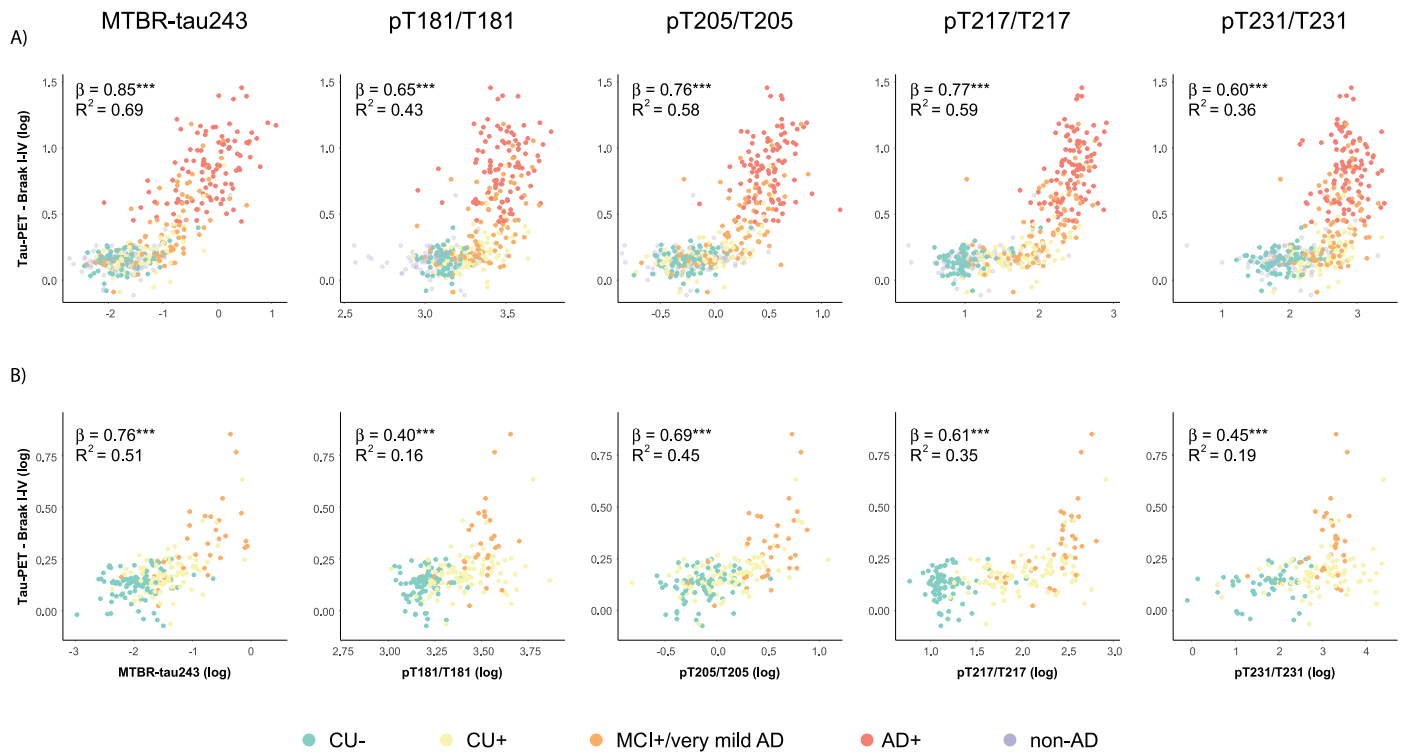
Extended Data Fig. 1 | CSF biomarkers by diagnosis. Levels of each CSF biomarkers by clinical diagnosis and amyloid status in the BioFINDER-2 cohort (n = 448). Amyloid-positive participants were selected based on CSF A β 42/40 (CSF A β 42/40 < 0.08). Larger pink dots represent two MAPT R406W mutation carriers (one CU- and the other in FTDP groups), both amyloid-negative but with substantial tau-PET binding. In boxplots, central band represents the median of the group, the lower and upper hinges correspond to the first and third quartiles, and the whiskers represent the maximum/minimum value or the 1.5 IQR from the hinge, whatever is lower). Differences in CSF biomarker levels by diagnostic groups were tested using ANCOVA adjusted for age and sex. Post

hoc analyses were performed two-sided using the Tuckey test. Actual p values are reported in Supplementary Table 1 for space reasons. p < 0.050; **, p < 0.010; ***, p < 0.001. Abbreviations: AD +, Alzheimer's disease dementia amyloid positive; CBS, corticobasal syndrome; CU-, cognitively unimpaired amyloid negative; CU+, cognitively unimpaired amyloid positive; FTDP, frontotemporal dementia; MCI+, mild cognitive impairment amyloid positive; MTBR, microtubule-binding region; PD, Parkinson's disease; PDD, Parkinson's disease dementia; PPA, primary progressive aphasia; PSP, progressive supranuclear palsy.



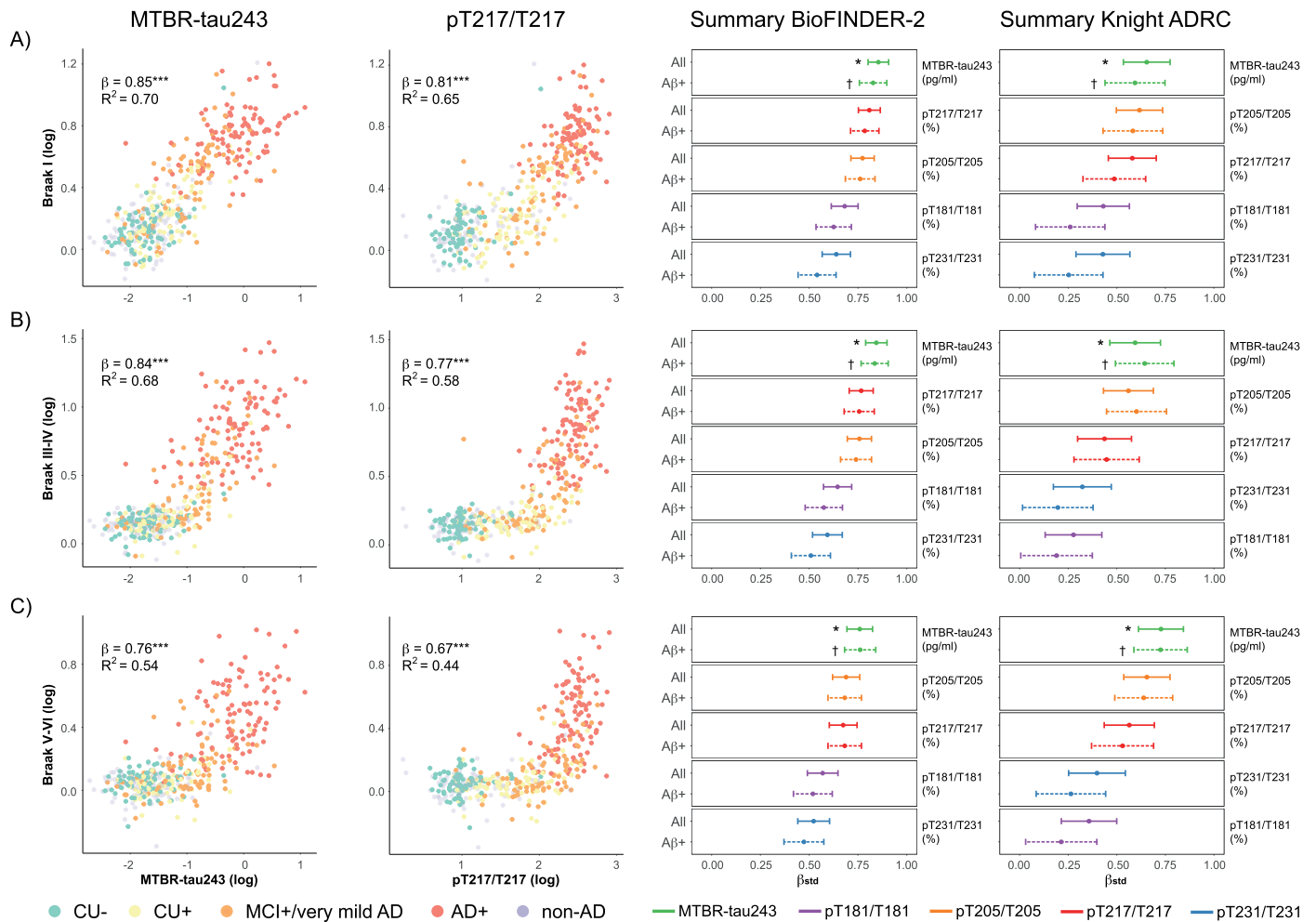
Extended Data Fig. 2 | Associations between all CSF biomarkers and A β -PET. Associations between CSF biomarkers and amyloid-PET (Centiloid) in BioFINDER-2 (A) and Knight ADRC (B) participants. Linear regression models, adjusting for age and sex, were used to obtain standardized β and p values shown in the plots. In the BioFINDER-2 cohort, orange dots represent MCI+ participants whereas in the Knight-ADRC cohort, represent very mild AD. *, $p < 0.050$;

** , $p < 0.010$; *** , $p < 0.001$. Abbreviations: AD + , Alzheimer’s disease dementia amyloid positive; CL, Centiloids, CSF, cerebrospinal fluid; CU- , cognitively unimpaired amyloid negative; CU + , cognitively unimpaired amyloid positive; MCI + , mild cognitive impairment amyloid positive; MTBR, microtubule binding region; non-AD, non-Alzheimer’s disease dementia; PET, positron emission tomography.



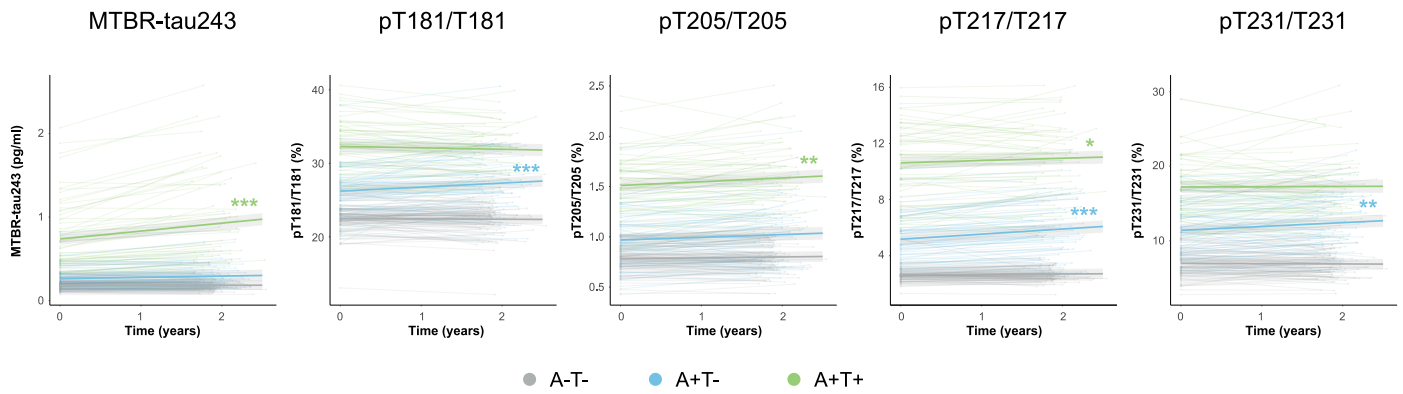
Extended Data Fig. 3 | Associations between all CSF biomarkers and tau-PET in the Braak I-IV ROI. Associations between CSF biomarkers and tau-PET in the Braak I-IV ROI (SUVR) in BioFINDER-2 (A) and Knight ADRC (B) participants. Linear regression models, adjusting for age and sex, were used to obtain standardized β and p-values shown in the plots. In the BioFINDER-2 cohort, orange dots represent MCI+ participants whereas in the Knight-ADRC cohort,

represent very mild AD. *, $p < 0.050$; **, $p < 0.010$; ***, $p < 0.001$. Abbreviations: AD+, Alzheimer's disease dementia amyloid positive; CSF, cerebrospinal fluid; CU-, cognitively unimpaired amyloid negative; CU+, cognitively unimpaired amyloid positive; MCI+, mild cognitive impairment amyloid positive; MTBR, microtubule binding region; non-AD, non-Alzheimer's disease dementia; PET, positron emission tomography, SUVR, standardized uptake value ratio.



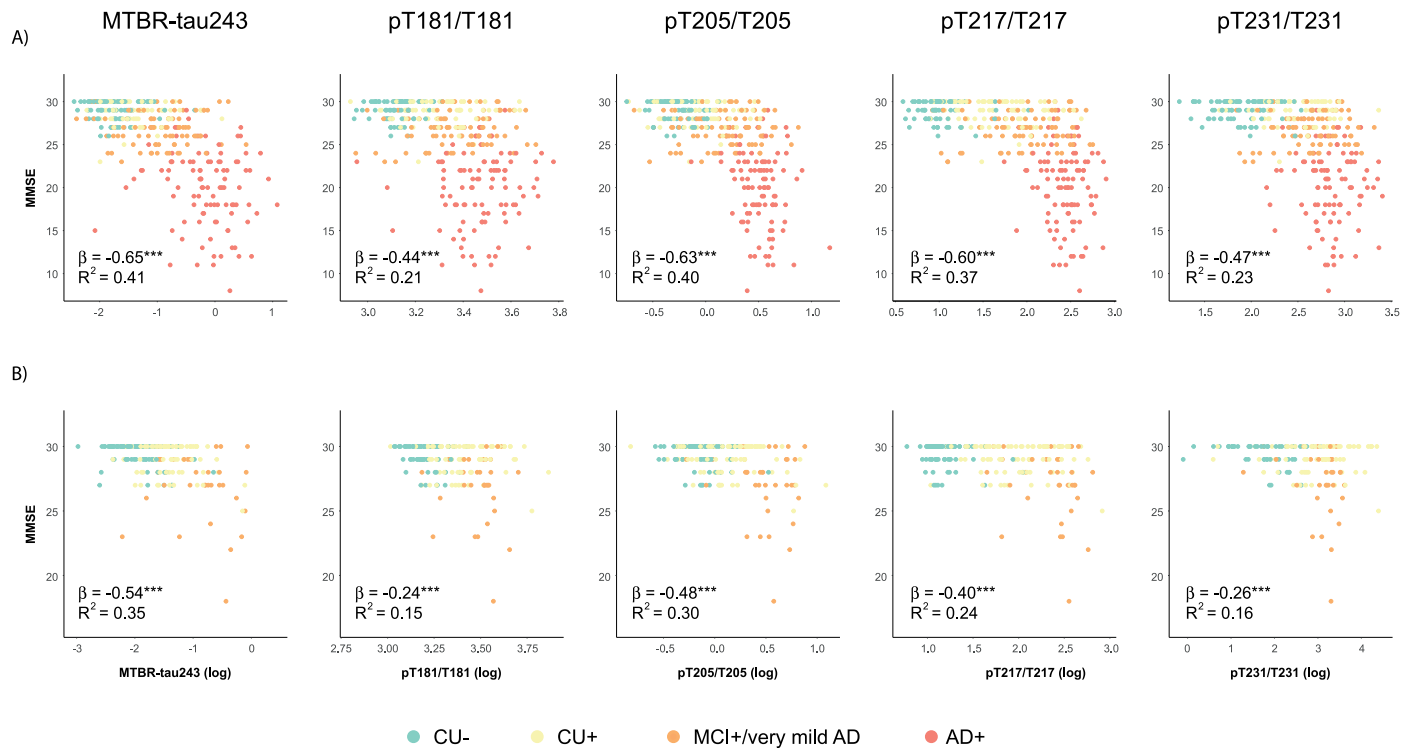
Extended Data Fig. 4 | Associations between CSF biomarkers and tau-PET in different Braak regions. Associations between CSF biomarkers and tau-PET in Braak I (A), Braak III–IV (B) and Braak V–VI (C) regions. First two columns show scatter-plots of MTBR-tau243 (first column) and pT217/T217 (second column) and tau-PET in BioFINDER-2 participants ($n = 443$), colored by diagnosis and amyloid status. Linear regression models, adjusting for age and sex, were used to obtain standardized β , p-values (asterisks) and R^2 shown in the plots. Third and fourth columns show standardized β of the association between each CSF biomarker and tau-PET in BioFINDER-2 and Knight ADRC participants ($n = 219$; except for pT231/T231 in which $n = 184$), respectively. Solid and dashed lines show standardized β (central dot) and 95%CI when all participants or only amyloid positive participants (BioFINDER-2: $n = 287$; Knight ADRC, $n = 136$) were included, respectively. Asterisks (crosses) show the highest or not significantly

different standardized β in all (amyloid positive only) participants, in each cohort and outcome. Amyloid-positive participants were selected based on CSF A β 42/40 previously validated cutoffs (CSF A β 42/40 < 0.08 in BioFINDER-2 and CSF A β 42/40 < 0.0673 in Knight ADRC). Association p-values were based on two-sided tests and bootstrapping p-values from one-sided tests, all unadjusted for multiple comparisons. All p-values from associations between CSF biomarkers and tau-PET shown in the scatter-plots were < 0.001. *, $p < 0.050$; **, $p < 0.010$; ***, $p < 0.001$. Abbreviations: A β +, amyloid positive; AD +, Alzheimer’s disease dementia amyloid positive; CSF, cerebrospinal fluid; CU-, cognitively unimpaired amyloid negative; CU +, cognitively unimpaired amyloid positive; MCI +, mild cognitive impairment amyloid positive; MTBR, microtubule binding region; non-AD, non-Alzheimer’s disease dementia; PET, positron emission tomography; SUVR, standardized uptake value ratio.



Extended Data Fig. 5 | Longitudinal CSF biomarkers trajectories by baseline “A” and “T” status. Individual (shaded lines) and group (bold lines) CSF biomarker levels trajectories over time based on their A/T baseline status. Statistical differences to the reference group (A-T-) are shown with asterisks with the appropriate color. Longitudinal CSF data was only available in BioFINDER-2. Amyloid-positive participants were selected based on a CSF A β 42/40 previously

validated cutoff (CSF A β 42/40 < 0.08). Tau positivity was assessed based on tau-PET SUVR in the meta-ROI (Braak I-IV SUVR > 1.32). *, $p < 0.050$; **, $p < 0.010$; ***, $p < 0.001$. Abbreviations: A-T-, amyloid and tau negative; A + T-, amyloid positive and tau negative; A + T+, amyloid positive, tau positive; CSF, cerebrospinal fluid; MTBR, microtubule binding region; PET, positron emission tomography.

**Extended Data Fig. 6 | Associations between all CSF biomarkers and MMSE.**

In BioFINDER-2 cohort (A), orange dots represent MCI+ participants whereas in the Kingst-ADRC cohort (B), represent very mild AD. Linear regression models, adjusting for age, sex and years of education were used to obtain standardized β and p-values shown in the plots. *, $p < 0.50$; **, $p < 0.010$; ***, $p < 0.001$.

Abbreviations: AD +, Alzheimer's disease dementia amyloid positive; CSF,

cerebrospinal fluid; CU-, cognitively unimpaired amyloid negative; CU+, cognitively unimpaired amyloid positive; MCI+, mild cognitive impairment amyloid positive; MMSE, Mini Mental State Examination; MTBR, microtubule binding region; PET, positron emission tomography, SD, standard deviation; SUVR, standardized uptake value ratio.

Extended Data Table 1 | Knight ADRC participants characteristics

Characteristic	All		CU-		CU+		Very mild AD		AD+	
	n=	219	n=	83	n=	88	n=	35	n=	13
Demographics										
Age, years	219	71.2 (6.55)	83	68.5 (6.55)	88	71.4 (11.3)	35	75.5 (6.55)	13	74.9 (7.2)
Women, n (%)	219	112, 51.1%	83	39, 47.0%	88	50, 56.8%	35	17, 48.6%	13	6, 46.2%
Race (Black/White/Other), n (%)	219	9/206/4	83	7/76/0	88	2/83/3	35	0/34/1	13	0/13/0
APOE-ε4 carriers, n (%)	217	96, 43.8%	83	17, 20.4%	87	49, 56.3%	34	22, 64.7%	13	8, 61.5%
Years of education	219	16.3 (2.81)	83	16.6 (2.81)	88	16.4 (2.39)	35	15.4 (2.81)	13	15.5 (2.7)
CSF Aβ measures										
CSF Aβ42/Aβ40	219	0.0574 (0.0094)	83	0.0895 (0.0094)	88	0.0481 (0.0182)	35	0.0447 (0.0094)	13	0.0378 (0.0123)
CSF Aβ42/40 positivity, n (%)	219	136 (62.1%)	83	0 (0%)	88	88 (100%)	35	35 (100%)	13	13 (100%)
Amyloid- and tau-PET measures										
Amyloid-PET Centiloid	219	41.8 (28)	83	9.17 (28)	88	48.6 (29.7)	35	77.9 (28)	13	107 (37.1)
Amyloid-PET status (n, % positive)	219	123, 56.2%	83	4, 4.8%	88	72, 81.8%	35	34, 97.1%	13	13, 100%
Interval between LP and amyloid-PET	219	0.115 (0.29)	83	0.101 (0.29)	88	0.0986 (0.214)	35	0.14 (0.29)	13	0.186 (0.222)
Tau-PET Braak I-IV, SUVR	219	1.18 (0.289)	83	1.14 (0.289)	88	1.19 (0.102)	35	1.31 (0.289)	13	1.57 (0.526)
Tau-PET positivity, n (%)	219	36, 16.4%	83	0, 0%	88	6, 6.8%	35	17, 48.6%	13	13, 100%
Interval between LP and tau-PET (years)	219	0.112 (0.17)	83	0.112 (0.17)	88	0.11 (0.203)	35	0.164 (0.17)	13	0.0821 (0.257)
CSF tau by mass spectrometry										
pT181/T181 (%)	219	27.8 (4.31)	83	24.5 (4.31)	88	29.9 (6.57)	35	33.7 (4.31)	13	31.8 (4.37)
pT205/T205 (%)	219	1.04 (0.65)	83	0.87 (0.65)	88	1.08 (0.46)	35	1.65 (0.65)	13	1.98 (0.54)
pT217/T217 (%)	219	5.78 (4.84)	83	3.06 (4.84)	88	7.68 (4.77)	35	11.5 (4.84)	13	12.9 (3.14)
pT231/T231 (%)	184	14.7 (8.13)	64	4.76 (8.13)	78	22.2 (19.6)	31	25.5 (8.13)	8	41.2 (17.4)
MTBR-tau243 (pg/ml)	219	0.207 (0.35)	83	0.14 (0.35)	88	0.23 (0.116)	35	0.451 (0.35)	13	0.701 (0.335)
Cognitive Measures										
MMSE	219	28.5 (2.73)	83	29.5 (2.73)	88	29.2 (1.12)	35	27.1 (2.73)	13	22.2 (3.18)

Abbreviations: AD+, Alzheimer's disease dementia amyloid positive; CSF, cerebrospinal fluid; CU-, cognitively unimpaired amyloid negative; CU+, cognitively unimpaired amyloid positive; MMSE, Mini-Mental State Examination; MTBR, microtubule binding region; PET, positron emission tomography; SUVR, standardized uptake value ratio. Parenthesis in rows: standard deviation.

Extended Data Table 2 | Associations between CSF biomarkers and A β -PET and tau-PET

Biomarker	β std[95%CI]	BioFINDER-2			Knight ADRC			
		p (β)	p (comp.)	R^2	β std[95%CI]	p (β)	p (comp.)	R^2
All participants								
Aβ-PET								
pT181/T181	0.66 [0.57, 0.75]	<0.001	<0.001	0.47	0.67 [0.56, 0.78]	<0.001	<0.001	0.47
pT205/T205	0.66 [0.57, 0.75]	<0.001	<0.001	0.47	0.69 [0.58, 0.80]	<0.001	<0.001	0.49
pT217/T217	0.81 [0.74, 0.88]	<0.001	Ref.	0.68	0.87 [0.79, 0.95]	<0.001	Ref.	0.74
pT231/T231	0.75 [0.68, 0.83]	<0.001	0.008	0.60	0.62 [0.51, 0.73]	<0.001	<0.001	0.45
MTBR-tau243	0.56 [0.46, 0.66]	<0.001	<0.001	0.33	0.61 [0.49, 0.74]	<0.001	<0.001	0.37
Aβ-positive participants								
pT181/T181	0.52 [0.39, 0.64]	<0.001	<0.001	0.32	0.46 [0.30, 0.63]	<0.001	<0.001	0.22
pT205/T205	0.62 [0.51, 0.74]	<0.001	0.088	0.45	0.62 [0.47, 0.76]	<0.001	0.074	0.37
pT217/T217	0.69 [0.59, 0.80]	<0.001	Ref.	0.53	0.71 [0.57, 0.84]	<0.001	Ref.	0.50
pT231/T231	0.62 [0.51, 0.74]	<0.001	0.035	0.45	0.53 [0.37, 0.68]	<0.001	<0.001	0.29
MTBR-tau243	0.46 [0.32, 0.59]	<0.001	<0.001	0.25	0.46 [0.29, 0.63]	<0.001	0.001	0.21
Tau-PET								
All participants								
pT181/T181	0.65 [0.58, 0.72]	<0.001	<0.001	0.43	0.40 [0.26, 0.54]	<0.001	<0.001	0.16
pT205/T205	0.76 [0.70, 0.82]	<0.001	<0.001	0.58	0.69 [0.57, 0.80]	<0.001	0.085	0.45
pT217/T217	0.77 [0.71, 0.83]	<0.001	<0.001	0.59	0.61 [0.49, 0.73]	<0.001	<0.001	0.35
pT231/T231	0.60 [0.52, 0.68]	<0.001	<0.001	0.36	0.45 [0.31, 0.59]	<0.001	<0.001	0.19
MTBR-tau243	0.85 [0.80, 0.90]	<0.001	Ref.	0.69	0.76 [0.65, 0.87]	<0.001	Ref.	0.51
Aβ-positive participants								
pT181/T181	0.58 [0.49, 0.68]	<0.001	<0.001	0.34	0.25 [0.07, 0.43]	0.007	<0.001	0.05
pT205/T205	0.74 [0.67, 0.82]	<0.001	0.001	0.55	0.67 [0.52, 0.81]	<0.001	0.092	0.42
pT217/T217	0.76 [0.69, 0.84]	<0.001	0.001	0.58	0.58 [0.43, 0.73]	<0.001	0.001	0.32
pT231/T231	0.51 [0.41, 0.61]	<0.001	<0.001	0.27	0.31 [0.13, 0.48]	0.001	<0.001	0.08
MTBR-tau243	0.84 [0.77, 0.91]	<0.001	Ref.	0.67	0.76 [0.63, 0.89]	<0.001	Ref.	0.53

Linear regression models were used to assess the associations between CSF biomarkers and amyloid-PET (Centiloids) and tau-PET (SUVR) in Braak I-IV ROI adjusting for age and sex. Amyloid-positive participants were selected based on CSF A β 42/40 previously validated cutoffs (CSF A β 42/40 < 0.08 in BioFINDER-2 and CSF A β 42/40 < 0.0673 in Knight ADRC). P comparison (p comp.) was calculated to assess differences between the strongest association (Ref.) and each of the other CSF biomarkers using bootstrapping ($n=500$) from adjusted β . Significant p comparison (<0.05) suggests weaker associations. Abbreviations: A β , amyloid; CI, confidence interval; CSF, cerebrospinal fluid; MTBR, microtubule binding region; PET, positron emission tomography; SUVR, standardized uptake value ratio.

Extended Data Table 3 | Proportion of variation of CSF biomarker levels explained by amyloid and tau

Biomarker	BioFINDER-2							Knight ADRC						
	pR ² A β	ppR ² A β (%)	pR ² Tau	ppR ² Tau (%)	R ²	Δ R ²	p	pR ² A β	ppR ² A β (%)	pR ² Tau	ppR ² Tau (%)	R ²	Δ R ²	p
Amyloid-PET														
pT181/T181	0.32	55.7%	0.13	22.0%	0.58	-0.19	0.006	0.25	70.1%	0.02	4.9%	0.36	-0.24	0.003
pT205/T205	0.29	45.5%	0.25	39.7%	0.64	-0.04	0.657	0.27	45.2%	0.27	45.4%	0.59	0.00	0.990
pT217/T217	0.57	74.7%	0.19	24.7%	0.77	-0.38	<0.001	0.51	75.1%	0.14	19.9%	0.68	-0.38	<0.001
pT231/T231	0.46	76.0%	0.02	3.3%	0.6	-0.44	<0.001	0.31	68.8%	0.04	8.6%	0.45	-0.27	<0.001
MTBR-tau243	0.14	22.3%	0.38	60.6%	0.63	0.24	<0.001	0.09	16.0%	0.36	66.7%	0.54	0.27	<0.001
CSF Aβ42/40														
pT181/T181	0.33	52.9%	0.21	33.7%	0.62	-0.12	0.014	0.41	82.8%	0.02	3.5%	0.5	-0.39	<0.001
pT205/T205	0.13	19.6%	0.43	66.8%	0.64	0.3	<0.001	0.20	36.5%	0.32	57.6%	0.56	0.12	0.125
pT217/T217	0.54	66.6%	0.46	56.5%	0.82	-0.08	0.044	0.71	87.6%	0.23	28.0%	0.81	-0.48	<0.001
pT231/T231	0.46	69.8%	0.13	19.1%	0.67	-0.34	<0.001	0.51	84.0%	0.04	7.0%	0.61	-0.47	<0.001
MTBR-tau243	0.16	21.4%	0.55	75.1%	0.73	0.39	<0.001	0.20	33.5%	0.38	63.8%	0.59	0.18	0.014

Proportion of variation of CSF biomarker levels explained by amyloid and tau was calculated by partial R² (pR²) in multivariable linear regression models with amyloid (CSF A β 42/40 [top rows] or amyloid-PET [bottom rows]) and tau (tau-PET in Braak I-IV ROI) as predictors and each CSF biomarker as outcome, adjusting for age and sex. Percentual partial R² (ppR²) were calculated as the partial R² of each predictor divided by the total R² of the model (100 * pR²/R²). Δ R² represents the difference between amyloid and tau partial R², with positive values meaning more proportion of variance explained by tau (Δ R² tau - Δ R² A β). Differences on partial R² were assessed by bootstrapping, and significant p-values (p < 0.05, in bold) represent significant differences on the contribution of tau and amyloid pathologies on each of the CSF levels. Abbreviations: A β , amyloid; CSF, cerebrospinal fluid; MTBR, microtubule binding region.

Extended Data Table 4 | Parsimonious models for predicting AD-related continuous measures

Cohort	Predictor	pR ²	R ²	AICc
All participants				
Aβ-PET				
BioFINDER-2	pT205/T205	0.06	0.77	370.2
	pT217/T217	0.16		
	Aβ42/40	0.11		
Knight ADRC	pT205/T205	0.02	0.73	261.7
	pT217/T217	0.17		
	Aβ42/40	0.03		
Tau-PET – Braak I-IV region				
BioFINDER-2	pT205/T205	0.22	0.75	614.1
	MTBR-tau243	0.40		
Knight ADRC	pT205/T205	0.14	0.58	339.5
	MTBR-tau243	0.24		
MMSE				
BioFINDER-2	pT205/T205	0.1	0.48	754.6
	MTBR-tau243	0.12		
Knight ADRC	pT205/T205	0.05	0.34	415.2
	MTBR-tau243	0.11		
Aβ-positive participants				
Aβ-PET				
BioFINDER-2	pT205/T205	0.09	0.61	341
	pT217/T217	0.03		
	pT231/T231	0.02		
	Aβ42/40	0.01		
	Age	0.03		
Knight ADRC	pT205/T205	0.04	0.51	258.5
	pT217/T217	0.25		
Tau-PET – Braak I-IV region				
BioFINDER-2	pT205/T205	0.23	0.74	433.9
	MTBR-tau243	0.41		
Knight ADRC	pT205/T205	0.14	0.58	239.9
	MTBR-tau243	0.28		
MMSE				
BioFINDER-2	pT205/T205	0.09	0.41	609.9
	MTBR-tau243	0.12		
Knight ADRC	pT205/T205	0.04	0.36	291.1
	MTBR-tau243	0.13		
	Education	0.06		

Partial R² (pR²) for all predictors included in the parsimonious model were calculated in a multivariable linear regression model with amyloid-PET, tau-PET and MMSE continuous measures as outcomes, respectively. R² and AICc for the whole model are also included in the table. Parsimonious model for each outcome and cohort were obtained with the optimal combination of CSF biomarkers and demographics (age and/or sex and/or education) assessed using a LASSO regression. Non-AD cases were excluded from BioFINDER-2 cohort for the MMSE analyses. Amyloid-positive participants were selected based on CSF Aβ42/40 previously validated cutoffs (CSF Aβ42/40 < 0.08 in BioFINDER-2 and CSF Aβ42/40 < 0.0673 in Knight ADRC). Abbreviations: Aβ, amyloid; AICc, corrected Akaike information criterion; CSF, cerebrospinal fluid; LASSO, least absolute shrinkage and selection operator; MMSE, Mini-Mental State Examination; MTBR, microtubule binding region; PET, positron emission tomography.

Reporting Summary

Nature Portfolio wishes to improve the reproducibility of the work that we publish. This form provides structure for consistency and transparency in reporting. For further information on Nature Portfolio policies, see our [Editorial Policies](#) and the [Editorial Policy Checklist](#).

Statistics

For all statistical analyses, confirm that the following items are present in the figure legend, table legend, main text, or Methods section.

- | n/a | Confirmed |
|-------------------------------------|--|
| <input type="checkbox"/> | <input checked="" type="checkbox"/> The exact sample size (n) for each experimental group/condition, given as a discrete number and unit of measurement |
| <input type="checkbox"/> | <input checked="" type="checkbox"/> A statement on whether measurements were taken from distinct samples or whether the same sample was measured repeatedly |
| <input type="checkbox"/> | <input checked="" type="checkbox"/> The statistical test(s) used AND whether they are one- or two-sided
<i>Only common tests should be described solely by name; describe more complex techniques in the Methods section.</i> |
| <input type="checkbox"/> | <input checked="" type="checkbox"/> A description of all covariates tested |
| <input type="checkbox"/> | <input checked="" type="checkbox"/> A description of any assumptions or corrections, such as tests of normality and adjustment for multiple comparisons |
| <input type="checkbox"/> | <input checked="" type="checkbox"/> A full description of the statistical parameters including central tendency (e.g. means) or other basic estimates (e.g. regression coefficient) AND variation (e.g. standard deviation) or associated estimates of uncertainty (e.g. confidence intervals) |
| <input type="checkbox"/> | <input checked="" type="checkbox"/> For null hypothesis testing, the test statistic (e.g. F , t , r) with confidence intervals, effect sizes, degrees of freedom and P value noted
<i>Give P values as exact values whenever suitable.</i> |
| <input checked="" type="checkbox"/> | <input type="checkbox"/> For Bayesian analysis, information on the choice of priors and Markov chain Monte Carlo settings |
| <input checked="" type="checkbox"/> | <input type="checkbox"/> For hierarchical and complex designs, identification of the appropriate level for tests and full reporting of outcomes |
| <input type="checkbox"/> | <input checked="" type="checkbox"/> Estimates of effect sizes (e.g. Cohen's d , Pearson's r), indicating how they were calculated |

Our web collection on [statistics for biologists](#) contains articles on many of the points above.

Software and code

Policy information about [availability of computer code](#)

Data collection

NanoLC-MS/MS experiments were performed using nanoAcquity ultra-performance LC system (Waters) coupled to Orbitrap Tribrid Eclipse mass spectrometer (Thermo Scientific) operating in parallel reaction monitoring mode. MS transitions were extracted using Skyline v.22.2.0.255 (MacCoss lab, University of Washington).

Data analysis

Data were aggregated using Tableau v.2022.2.2 (Tableau Software) to calculate CSF biomarker levels. Differences in CSF biomarker levels were tested by diagnostic groups using ANCOVA adjusted for age and sex. Post-hoc analyses were performed using the Tuckey test. Linear regression models were used to assess the association between amyloid- and tau-PET (independent variable) and each of the CSF biomarkers (dependent variable), after adjusting for age and sex. For cognition, education was also used as covariate in the linear regression models. All standardized betas were compared to the highest for each outcome and cohort, by building a distribution of the betas' difference and using that to infer significance using a bootstrapping approach ($n=500$) with the boot package. Proportion of variation of CSF levels by amyloid and tau measures were assessed using linear regression models with both amyloid and tau as predictors, CSF levels as outcomes and age and sex as covariates. The partial R^2 of amyloid and tau, raw and as a percentage of the total R^2 of the model were calculated using the rsq package. This was used as a measure of proportion of variance explained by amyloid and tau. Next, prediction of amyloid and tau continuous measures was assessed with linear regression models, where amyloid- and tau-PET measures were used as outcomes in independent models and individual CSF biomarkers as predictors. A basic model was also created with only covariates (age and sex) as predictors. Additionally, a parsimonious model was constructed to optimally predict (highest accuracy with lower number of predictors) each of these measures, independently for each cohort. To this aim, LASSO regression models were used (glmnet package), initially including all CSF biomarkers and covariates. Only those predictors selected by the LASSO regression and with a significant contribution ($p < 0.1$) in the model were finally included in the parsimonious model. Similar methods were used for predicting cognition (MMSE in the two cohorts and CDR in Knight ADRC) additionally including education as covariate. In these cases, the parsimonious model was compared to one including only tau-PET as predictor. F-tests were used to compare nested models (including the same subset of predictors). When comparing models with different

predictors we used the Vuong's test using the nonnest2 package. Finally, CSF longitudinal changes by baseline amyloid and tau status were assessed in the BioFINDER-2 cohort. Individual participant slopes were calculated using linear regression models to calculate rate of change differences and compare them between groups using a Kruskal-Wallis test. Further, we created group trajectories with linear mixed models using the lme4 package for visualization. Here, CSF biomarkers were used as outcome, interaction between time and baseline amyloid and tau status as predictor and age and sex main effects as covariates, using random intercepts and fixed time-slopes due to low number of time points. CSF and amyloid- and tau-PET measures were log-transformed in linear regression analyses. A two-sided P value <0.05 was considered statistically significant. R version 4.1.0 was used for all statistical analyses.

For manuscripts utilizing custom algorithms or software that are central to the research but not yet described in published literature, software must be made available to editors and reviewers. We strongly encourage code deposition in a community repository (e.g. GitHub). See the Nature Portfolio [guidelines for submitting code & software](#) for further information.

Data

Policy information about [availability of data](#)

All manuscripts must include a [data availability statement](#). This statement should provide the following information, where applicable:

- Accession codes, unique identifiers, or web links for publicly available datasets
- A description of any restrictions on data availability
- For clinical datasets or third party data, please ensure that the statement adheres to our [policy](#)

The datasets generated and/or analyzed during the current study are available from the corresponding authors (R.J.B and O.H). We will share datasets within the restrictions of IRB ethics approvals, upon reasonable request. Pseudonymized data from the BioFINDER-2 will be shared by request from a qualified academic investigator for the sole purpose of replicating procedures and results presented in the article and as long as data transfer is in agreement with EU legislation on the general data protection regulation and decisions by the Ethical Review Board of Sweden and Region Skåne, which should be regulated in a material transfer agreement. Knight ADRC data are available to qualified investigators who have a proposal approved by an institutional committee (<https://knightadrc.wustl.edu/Research/ResourceRequest.htm>) that meets monthly. The study must be approved by an institutional review board to ensure ethical research practices and investigators must agree to the terms and conditions of the data use agreement, which includes not distributing the data without permission.

Human research participants

Policy information about [studies involving human research participants and Sex and Gender in Research](#).

Reporting on sex and gender

Sex and race were self-identified.

Population characteristics

The BioFINDER-2 cohort included 448 individuals, the majority of whom had cognitive impairment (281, 63%): 81 cognitively unimpaired Amyloid negative (CU-), 79 cognitively unimpaired Amyloid positive (CU+), 90 Amyloid positive with mild cognitive impairment (MCI+), 102 Amyloid positive with AD dementia (AD+) and 96 with other dementias (non-AD). The average age was 70.9 ± 8.4 years (mean \pm standard deviation), 221 (49.3%) were women, and 258 (57.6%) were APOE $\epsilon 4$ carriers. The Knight ADRC cohort included 219 individuals, most of whom were cognitively unimpaired (171, 78%): 83 CU-, 88 CU+, 35 very mild AD, and 13 AD+. The average age was 71.2 ± 6.6 years, 112 (51.1%) were women, and 96 (43.8%) were APOE $\epsilon 4$ carriers.

Recruitment

Participants were included from two cohorts: the Swedish BioFINDER-2 (NCT03174938) at Lund University (Lund, Sweden), and the Knight ADRC from Washington University (St Louis, MO, USA). BioFINDER-2 cohort included cognitively unimpaired participants (recruited as cognitively normal controls or as subjective cognitive decline [SCD] patients), patients with MCI, AD dementia patients and patients with a non-AD neurodegenerative disease. Participants were recruited at Skåne University Hospital and the Hospital of Ängelholm in Sweden. Details on recruitment, exclusion and inclusion criteria have been presented before (reference 11). All participants underwent lumbar puncture at baseline and at the follow-up after two years for CSF sampling. Participants underwent cognitive testing, including MMSE. The Knight ADRC cohort consisted of community-dwelling volunteers enrolled in studies of memory and aging at Washington University in St. Louis. All Knight ADRC participants underwent a comprehensive clinical assessment that included a detailed interview of a collateral source, a neurological examination of the participant, the Clinical Dementia Rating (CDR) and the MMSE. Individuals with a CDR of 0.5 or greater were considered to have a dementia syndrome and the probable aetiology of the dementia syndrome was formulated by clinicians based on clinical features in accordance with standard criteria and methods.

Ethics oversight

All participants in the Swedish BioFINDER-2 and the Knight ADRC cohorts gave written informed consent and ethical approvals were granted by the Regional Ethical Committee in Lund, Sweden and the Washington University Human Research Protection Office, respectively.

Note that full information on the approval of the study protocol must also be provided in the manuscript.

Field-specific reporting

Please select the one below that is the best fit for your research. If you are not sure, read the appropriate sections before making your selection.

- Life sciences Behavioural & social sciences Ecological, evolutionary & environmental sciences

For a reference copy of the document with all sections, see nature.com/documents/nr-reporting-summary-flat.pdf

Life sciences study design

All studies must disclose on these points even when the disclosure is negative.

Sample size	No statistical methods were used to pre-determine sample sizes but our sample sizes are similar or larger to those used for similar studies. (e.g., Mila-Aloma, M., et al. Nat Med 28, 1797-1801 (2022) and Barthelemy, N.R., et al. Nat Med 26, 398-407 (2020))
Data exclusions	No data points were excluded from analyses; outliers were not removed.
Replication	We replicated our key findings in two large independent cohorts (BioFINDER-2 and Knight ADRC) with significant differences in demographics and using different PET tracers.
Randomization	Samples were randomized by groups such as cognitively unimpaired participants, patients with MCI, AD dementia patients and patients with a non-AD neurodegenerative disease. All samples had a random code as an identifier and researchers who performed experiments were blinded towards the code when performing the analyses.
Blinding	All assays and data extraction steps were performed by operators blinded to any clinical or biomarker information.

Reporting for specific materials, systems and methods

We require information from authors about some types of materials, experimental systems and methods used in many studies. Here, indicate whether each material, system or method listed is relevant to your study. If you are not sure if a list item applies to your research, read the appropriate section before selecting a response.

Materials & experimental systems

n/a	Involved in the study
<input type="checkbox"/>	<input checked="" type="checkbox"/> Antibodies
<input checked="" type="checkbox"/>	<input type="checkbox"/> Eukaryotic cell lines
<input checked="" type="checkbox"/>	<input type="checkbox"/> Palaeontology and archaeology
<input checked="" type="checkbox"/>	<input type="checkbox"/> Animals and other organisms
<input type="checkbox"/>	<input checked="" type="checkbox"/> Clinical data
<input checked="" type="checkbox"/>	<input type="checkbox"/> Dual use research of concern

Methods

n/a	Involved in the study
<input checked="" type="checkbox"/>	<input type="checkbox"/> ChIP-seq
<input checked="" type="checkbox"/>	<input type="checkbox"/> Flow cytometry
<input checked="" type="checkbox"/>	<input type="checkbox"/> MRI-based neuroimaging

Antibodies

Antibodies used	Tau1 (generated by Dr. Nicholas Kanaan) and HJ series (clone name: HJ8.5, HJ8.7, HJ32.11, and HJ34.8) antibodies (generated by Dr. David Holtzman) were used. For all antibodies, 3 mg/gram sepharose beads were generated. For Tau1 immunoprecipitation (IP), 1.1 ug antibody/sample was used. For HJ8.5 and HJ8.7 IP, 2.3 ug antibody/sample was used. For HJ32.11 and HJ34.8 IP, 11.25 ug antibody/sample was used.
Validation	Tau1, HJ8.5 and HJ8.7 were validated in the following studies. 1. Barthelemy NR, Toth B, Manser PT, et al. Site-Specific Cerebrospinal Fluid Tau Hyperphosphorylation in Response to Alzheimer's Disease Brain Pathology: Not All Tau Phospho-Sites are Hyperphosphorylated. Journal of Alzheimer's disease : JAD 2022; 85(1): 415-29. 2. Sato C, Barthelemy NR, Mawuenyega KG, et al. Tau Kinetics in Neurons and the Human Central Nervous System. Neuron 2018; 98(4): 861-4. HJ32.11 and HJ34.8 were newly generated antibodies and we confirmed that immunoprecipitation procedures using these antibodies worked well by the two replicate cohorts analyses.

Clinical data

Policy information about [clinical studies](#)

All manuscripts should comply with the ICMJE [guidelines for publication of clinical research](#) and a completed [CONSORT checklist](#) must be included with all submissions.

Clinical trial registration	BioFINDER-2 (NCT03174938) Knight ADRC (N/A--the study is NOT a clinical trial)
Study protocol	BioFINDER-2 (NCT03174938, https://clinicaltrials.gov/ct2/show/NCT03174938) Knight ADRC (N/A--the study is NOT a clinical trial)
Data collection	Data was obtained from CSF collected from participants in the BioFINDER-2 cohort (NCT03174938) including cognitively unimpaired participants, patients with MCI, AD dementia patients and patients with a non-AD neurodegenerative disease. The participants from the prospective Swedish BioFINDER-2 study were recruited at the Memory and Neurology clinics of Skåne University Hospital and the

Memory clinic of Ångelholm's Hospital in Sweden (dates of enrollment, February 2017-April 2021). Participants in the Knight ADRC cohort were community-dwelling volunteers enrolled in studies of memory and aging.

Outcomes

Main outcomes of the study included amyloid- and tau-PET, as well as cognition, assessed with MMSE. Amyloid-PET was measured in a neocortical meta-ROI using cerebellar grey as a reference region. Tau-PET SUVRs were calculated using the inferior cerebellum cortex as reference region and binding from a temporal meta-ROI were used for main analyses. Tau-PET SUVRs in Braak I, Braak III-IV and Braak V-VI were also assessed as secondary outcomes.